PARAMETRIC STUDY OF CATALYTIC CO HYDROGENATION FOR PRODUCING DIMETHYL ETHER

by

Hatice Merve Can

B.S., Chemical Engineering, Izmir Institute of Technology, 2013

M.S., Fuel and Energy Technologies, Boğaziçi University, 2015

Submitted to the Institute for Graduate Studies in
Science and Engineering in partial fulfillment of
the requirements for the degree of
Master of Science

Graduate Program in Chemical Engineering

Boğaziçi University

2016

to my family

ACKNOWLEDGEMENTS

First of all, I would like to express my truthful gratitude to my thesis supervisor Prof. Ahmet Kerim Avcı for his guidance, encouragement and trust in me. It was really a privilege to work with him during my thesis. I also want to thank him for his kindly attitude and support in every expect. I am very grateful to my co-supervisor Prof. Zeynep İlsen Önsan for her suggestions,help and emotional support for this study and future life. I learned a lot from her wisdom and experiences in catalysis and reaction engineering.

My sincere gratitude is due to my thesis committee members; Assoc. Prof. Hasan Bedir, Assoc. Prof. Alper Uzun and Prof. Ramazan Yıldırım for spending their valuable time to read and comment on my thesis.

Heartfelt thanks goes to my father, Ali Can, who I admire the most in my life and never give up trusting me in my endevours.I owe special thanks to my mother and brother for their endless love and prayers.

Very special thanks goes to my colleague and best friend Merve Demir for her encouragment and friendship not only for this thesis but also in my personal life. I would like to thank to my friends Bahar Kesim and Özgü Özer for their help and accompanies during my master years.

I would like thank my lab mates, Sinan Koç, Amin Delparish, Pelinsu Bulutoğlu and Begüm Koca. I was very lucky to work with the CATREL team, especially Melek Selcen Başar, Aybüke Leba, Çağla Uzunoğlu and Merve Eropak and I would like to thank all team members for their support.

Cordial thanks are for Bilgi Dedeoğlu for his technical assistance and also Melike Gürbüz, Başak Ünen and Yakup Bal for their friendly attitude. I cannot pass without presenting my sincere thanks to Andrew Musset from Autoclave Engineers for his great contribution during the commisioning of this project.

Last but not least, I would like to present my deepest thanks to Eray Özdemir for his tireless encouragement and emotional support not only for this project but also for my life. I would also like to acknowledged Boğaziçi Scientific Research Coodrination (BAP) through projects 6188 and 12100.

ABSTRACT

PARAMETRIC STUDY OF CATALYTIC CO HYDROGENATION FOR PRODUCING DIMETHYL ETHER

The objective of this study is to examine the catalytic performance of bi-functional catalyst systems in direct synthesis of dimethyl ether (DME). Direct synthesis method involves two consecutive steps: methanol synthesis followed by methanol dehydration. Hence, a commercial methanol synthesis catalyst (Cu-Zn based HiFuel-R120) was coupled with different methanol dehydration catalysts in a dual-bed micro-reactor. Methanol dehydration catalysts were prepared by incipient-to-wetness impregnation by varying CeO_2 loading on δ-Al_2O_3. Syngas-to-DME performance of the bi-functional catalyst system was studied in an Autoclave Engineers' BTRS-Jr-PC high-pressure, high-temperature reaction test system with a down-flow fixed-bed reactor designed to operate up to 600^oC and 100 atm. Temperature, pressure, feed composition and CeO_2 loading were tested for their effects on catalyst performance expressed in terms of CO conversion; DME, methane, carbon dioxide and methanol yields, and DME selectivity. Temperatures of 250, 275 and 300^oC and pressures of 25 and 34 bar were tested with CeO_2 loadings of 5%, 10% and 20% CeO_2 on δ-Al_2O_3 for methanol dehydration. Results on 5% and 10% CeO_2/δ-Al_2O_3 catalysts indicate that increasing the temperature enhances CO conversion and increases both DME selectivity and DME yield, while CO conversion on 20% CeO_2/δ-Al_2O_3 is not altered, which may be due to metal sintering. Increasing the pressure leads to higher catalytic activity on 5% and 10% CeO_2/δ-Al_2O_3, due to Le Chatelier's principle operative in methanol synthesis. Effect of H_2/CO molar feed ratio on CO conversion and DME selectivity is studied at ratios of 1 and 2, and results show that a H_2-rich medium increases DME selectivity. Effect of decreasing CeO_2 loading is to enhance CO conversion and DME selectivity. Highest CO conversion (36.6%) and DME selectivity (74.4%) are obtained when HiFUEL R120 is coupled with 5% CeO_2/δ-Al_2O_3 at 300 $^\circ$C and 34 bar using a H_2/CO molar feed ratio of 2.

ÖZET

KATALİTİK KARBON MONOKSİT HİDROJENASYONU DİMETİL ETER ÜRETİMİNİN PARAMETRİK İNCELENMESİ

Bu çalışmanın amacı, doğrudan dimetil eter (DME) sentezlenmesinde kullanılan çift-işlevli katalizör sistemlerinin performansını incelemekti. Doğrudan sentezleme yöntemi iki ardışık adımdan oluşur: metanol sentezi ve onu izleyen metanol dehidrasyonu. Bu amaçla, ticari metanol sentez katalizörü (Cu-Zn bazlı HiFuel-R120) ile farklı metanol dehidrasyon katalizörleri çift-yataklı bir mikroreaktörde birlikte kullanıldı. δ-Al_2O_3 taşıyıcıya yüklenen CeO_2 oranı değiştirilerek üç farklı metanol dehidrasyon katalizörü ıslak emdirme yöntemiyle hazırlandı. Çift-işlevli katalizör sistemiyle sentez gazından DME üretimi, 600 ^oC ve 100 atm kadar çıkabilen yüksek-basınçlı yüksek-sıcaklıklı Autoclave Engineers' BTRS Jr-PC reaksiyon test sisteminde aşağı-akışlı, sabit-yataklı borusal reaktör kullanılarak incelendi. Deneysel parametre olarak sıcaklık, basınç, girdi bileşimi ve yüklü CeO_2 oranı seçildi; katalizör performansının ölçüsü CO dönüşme yüzdesi; DME, metan, karbon dioksit, metanol verimleri, ve DME seçimliliği olarak alındı. Deneyler 250, 275 ve 300 ^oC sıcaklıkta, 25 ve 34 atm basınç eşliğinde, ağırlıkça %5, %10 veya %20 CeO_2 yüklü δ-Al_2O_3 metanol dehidrasyon katalizörüyle yapıldı. %5 ve %10 CeO_2 yüklü δ-Al_2O_3 ile elde edilen veriler, CO dönüşme yüzdesinin ve DME seçimliliğinin sıcaklıkla arttığını, %20 CeO_2 yüklü δ-Al_2O_3 ile CO dönüşmesinde bir fark olmadığını, bunun metal sinterleşmesine bağlanabileceğini gösterdi. %5 ve %10 CeO_2 yüklü δ-Al_2O_3 katalizörlerin etkinliklerinin basınçla arttığı, bu artışın metanol sentezi için geçerli Le Chatelier's ilkesine dayandığı görüldü. Girdideki molar H_2/CO oranı 1 veya 2 olan deneyler ile DME seçimliliğinin hidrojence zengin ortamda arttığı belirlendi. Yüklü CeO_2 oranı azaldıkça CO dönüşme yüzdesinin ve DME seçimliliğinin arttığı gözlendi. En yüksek CO dönüşme yüzdesi (%36) ve DME seçimliliği (%74.4), 300^oC sıcaklık ve 34 atm basınçta, H_2/CO oranı 2 olan girdi bileşimiyle ve metanol sentez katalizörü HiFuel-R120'nin %5 CeO_2/δ-Al_2O_3 metanol dehidrasyon katalizörü ile birlikte kullanıldığı deneylerde elde edildi.

TABLE OF CONTENTS

ACKNOWLEDGEMENTS iv
ABSTRACT vi
ÖZET vii
LIST OF FIGURES x
LIST OF TABLES xv
LIST OF SYMBOLS xvi
LIST OF ACRONYMS/ABBREVIATIONS xvii
1. INTRODUCTION 1
2. LITERATURE SURVEY 3
2.1. Dimethyl Ether as an Alternative Fuel 3
2.2. Properties of Dimethyl Ether 3
2.3. Environmental and Economic Impacts 6
2.4. Dimethyl Ether as Energy Carrier 6
2.5. Production of Dimethyl Ether 6
2.5.1. Indirect Synthesis Method 6
2.5.2. Direct Synthesis Method 7
2.6. Types of DME Reactors 8
2.7. Catalysts Used for DME Synthesis 8
2.7.1. Methanol Synthesis Catalysts 8
2.7.2. Methanol Dehydration Catalysts 10
2.8. Catalyst Preparation Methods 15
2.9. Factors Effecting The Activity of DME Synthesis Catalysts 18
2.9.1. Water Content 18
2.9.2. H_2/CO Molar Ratio 18
2.9.3. Operating Conditions 19
3. EXPERIMENTAL WORK 27
3.1. Materials 27
3.1.1. Chemicals 27

3.1.2. Gases and Liquids 27
3.2. Experimental Systems 28
3.2.1. Catalyst Preparation Systems 28
3.2.2. Catalyst Testing Systems 30
3.2.2.1. Feed Preparation Section 30
3.2.2.2. Reactor Section 33
3.2.2.3. Gas-Liquid Separator 34
3.2.2.4. Back Pressure Regulator 35
3.2.2.5. Gas Chromatography (GC) Sampling Valve 35
3.2.2.6. Transfer Lines 36
3.2.2.7. System Monitoring and Control 36
3.2.3. System Commissioning and Experimental Procedure 36
3.2.3.1. Troubleshooting and Commissioning 36
3.2.3.2. Experimental Procedure. 38
3.2.4. Product Analysis Systems. 40
4. RESULTS AND DISCUSSIONS. 46
4.1. Effect of Temperature 46
4.2. Effect of Pressure 56
4.3. Effect of Feed Composition 61
4.4. Effect of Catalyst Loading 66
5. CONCLUSION 70
5.1. Conclusions 70
5.2. Recommendations 71
REFERENCES 73
APPENDIX A: SAMPLE CONVERSION, SELECTIVITY AND YIELD CALCULATIONS 83

LIST OF FIGURES

Figure 2.1. Structure of dimethyl ether. 4

Figure 2.2. Process diagram for DME production. 7

Figure 3.1. Schematic diagram of impregnation system. 30

Figure 3.2. Preparation steps of $CeO_2/\delta\text{-}Al_2O_3$ catalyst via incipient to wetness impregnation. 31

Figure 3.3. The Autoclave Engineer's BTRS-Jr-PC high-pressure fixed bed reactor system. 32

Figure 3.4. The Autoclave Engineer's BTRS-Jr-PC reactor oven cabinet. 32

Figure 3.5. Flow sheet of the automated fixed bed reactor of BTRS-Jr-PC. 33

Figure 3.6. Screenshot of the HMI software used to control Autoclave Engineer's BTRS-Jr-PC. 34

Figure 3.7. GC sampling valve configurations. 35

Figure 3.8. Loading method for the tubular reactor. 39

Figure 4.1. Effect of temperature on catalytic performance on HiFUEL R120-5% $CeO_2/\delta\text{-}Al_2O_3$ ($CO/H_2/N_2$=32/64/4, 34 bar). 48

Figure 4.2. Temperature dependence of CO conversion with time-on-stream for HiFUEL R120-5% $CeO_2/\delta\text{-}Al_2O_3$ ($CO/H_2/N_2$=32/64/4, 34 bar). 48

Figure 4.3. Temperature dependence of DME, methanol, CH_4 and CO_2 selectivity for HiFUEL R120-5% CeO_2/δ-Al_2O_3 ($CO/H_2/N_2$=32/64/4, 34 bar). 49

Figure 4.4. Effect of temperature on catalytic performance on HiFUEL R120-10% CeO_2/δ-Al_2O_3 ($CO/H_2/N_2$=32/64/4, 34 bar). 50

Figure 4.5. Temperature dependence of CO conversion with time-on-stream for HiFUEL R120-10% CeO_2/δ-Al_2O_3 ($CO/H_2/N_2$=32/64/4, 34 bar). 51

Figure 4.6. Temperature dependence of DME, methanol, CH_4 and CO_2 selectivity for HiFUEL R120-10% CeO_2/δ-Al_2O_3 ($CO/H_2/N_2$=32/64/4, 34 bar). 51

Figure 4.7. Effect of temperature on catalytic performance on HiFUEL R120-20% CeO_2/δ-Al_2O_3 ($CO/H_2/N_2$=32/64/4, 34 bar). 54

Figure 4.8. Temperature dependence of DME, methanol, CH_4 and CO_2 selectivity for HiFUEL R120-20% CeO_2/δ-Al_2O_3 ($CO/H_2/N_2$=32/64/4, 34 bar). …. 54

Figure 4.9. Pressure dependence of CO conversion with time-on-stream for HiFUEL R120-5% CeO_2/δ-Al_2O_3 ($CO/H_2/N_2$=32/64/4, 275 and 300 °C). 57

Figure 4.10. Pressure dependence of DME, methanol, CH_4 and CO_2 selectivity for HiFUEL R120-5% CeO_2/δ-Al_2O_3 ($CO/H_2/N_2$=32/64/4, 275 and 300 °C). 57

Figure 4.11. Pressure dependence of CO conversion with time-on-stream for HiFUEL R120-10% CeO_2/δ-Al_2O_3 ($CO/H_2/N_2$=32/64/4, 275 and 300 °C). 59

Figure 4.12. Pressure dependence of DME, methanol, CH_4 and CO_2 selectivity for

HiFUEL R120-10% CeO_2/δ-Al_2O_3 ($CO/H_2/N_2$=32/64/4, 275 and 300 °C). 59

Figure 4.13. Feed composition (H_2/CO) dependence of CO conversion with time-on-stream for HiFUEL R120-5% CeO_2/δ-Al_2O_3 (34 bar, 300 °C). 63

Figure 4.14. Feed composition (H_2/CO) dependence of DME, methanol, CH_4 and CO_2 selectivity with time-on-stream for HiFUEL R120-5% CeO_2/δ-Al_2O_3(34 bar, 300 °C). 63

Figure 4.15. Feed composition (H_2/CO) dependence of CO conversion with time-on-stream for HiFUEL R120-10% CeO_2/δ-Al_2O_3 (34 bar, 300 °C). 64

Figure 4.16. Feed composition (H_2/CO) dependence of DME, methanol, CH_4 and CO_2 selectivity for HiFUEL R120-10% CeO_2/δ-Al_2O_3 (34 bar, 300 °C). 64

Figure 4.17. Comparison of catalytic activity of HiFUEL R120-5% CeO_2/δ-Al_2O_3, HiFUEL R120-10% CeO_2/δ-Al_2O_3 and HiFUEL R120-20% CeO_2/δ-Al_2O_3 at (a) 275 °C and (b) 300 °C ($CO/H_2/N_2$ =32/64/4, 34 bar). 67

Figure 4.18. Comparison of DME, methanol, CH_4 and CO_2 catalytic selectivity HiFUEL R120-5% CeO_2/δ-Al_2O_3, HiFUEL R120-10% CeO_2/δ-Al_2O_3 and HiFUEL R120-20% CeO_2/δ-Al_2O_3 at (a) 275 °C and (b) 300 °C ($CO/H_2/N_2$ =32/64/4, 34 bar). 68

Figure 4.19. Comparison of DME, methanol, CH_4 and CO_2 selectivity and CO Conversion (%) HiFUEL R120-5% CeO_2/δ-Al_2O_3, HiFUEL R120-10% CeO_2/δ-Al_2O_3 and HiFUEL R120-20% CeO_2/δ-Al_2O_3 at (a) 275 ^oC and (b) 300 ^oC ($CO/H_2/N_2$ =32/64/4, 34 bar). 69

LIST OF TABLES

Table 2.1. Comparison of chemical and physical properties of DME with some commonly used fuels. 5

Table 2.2. Production conditions in various studies on DME synthesis. 20

Table 3.1. Chemicals used for catalyst preparation. 27

Table 3.2. Applications and specifications of the liquids used. 27

Table 3.3. Applications and specifications of the gases used. 28

Table 3.4. Summary of the performed experiments and catalysts used. 40

Table 3.5. Properties of and analysis conditions used in Shimadzu GC-2014 unit. . 41

Table 3.6. Properties of and analysis conditions used in Shimadzu GCMS-QP2010. 42

Table 3.7. Total ionization cross section of the some compounds. 44

Table 4.1. Selectivity of main products with HiFUEL R120-5% CeO_2/δ-Al_2O_3 at 275 ^oC and 300 ^oC ($CO/H_2/N_2$ =32/64/4, 34 bar). 49

Table 4.2. Yield of main products with HiFUEL R120-5% CeO_2/δ-Al_2O_3 at 275 ^oC and 300 ^oC ($CO/H_2/N_2$ =32/64/4, 34 bar). 49

Table 4.3. Yield of by-products with HiFUEL R120-5% CeO_2/δ-Al_2O_3at 275 ^oC and 300 ^oC ($CO/H_2/N_2$ =32/64/4, 34 bar). 50

Table 4.4. Selectivity of main products with HiFUEL R120-10% $CeO_2/\delta\text{-}Al_2O_3$ at 275 and 300 ^oC ($CO/H_2/N_2$ =32/64/4, 34 bar). 52

Table 4.5. Yield of main products with HiFUEL R120-10% $CeO_2/\delta\text{-}Al_2O_3$ at 275 and 300 ^oC ($CO/H_2/N_2$ =32/64/4, 34 bar). 52

Table 4.6. Yield of by-products with HiFUEL R120-10% $CeO_2/\delta\text{-}Al_2O_3$at 275 and 300 ^oC ($CO/H_2/N_2$ =32/64/4, 34 bar). 52

Table 4.7. Selectivity of main products with HiFUEL R120-20% $CeO_2/\delta\text{-}Al_2O_3$ at 275 and 300 ^oC ($CO/H_2/N_2$ =32/64/4, 34 bar). 55

Table 4.8. Yield of main products with HiFUEL R120-20% $CeO_2/\delta\text{-}Al_2O_3$ at 275 and 300 ^oC ($CO/H_2/N_2$ =32/64/4, 34 bar). 55

Table 4.9. Yield of by-products with HiFUEL R120-20% $CeO_2/\delta\text{-}Al_2O_3$at 275 and 300 ^oC ($CO/H_2/N_2$ =32/64/4, 34 bar). 55

Table 4.10. Selectivity of main products with HiFUEL R120-5% $CeO_2/\delta\text{-}Al_2O_3$ at 25 and 34 bar ($CO/H_2/N_2$ =32/64/4, 34 bar). 58

Table 4.11. Yield of main products with HiFUEL R120-5% $CeO_2/\delta\text{-}Al_2O_3$ at 25 and 34 bar ($CO/H_2/N_2$ =32/64/4, 34 bar). 58

Table 4.12. Yield of by-products with HiFUEL R120-5% $CeO_2/\delta\text{-}Al_2O_3$at 25 and 34 bar ($CO/H_2/N_2$ =32/64/4, 34 bar). 58

Table 4.13. Selectivity of main products with HiFUEL R120-10 % $CeO_2/\ \delta\text{-}Al_2O_3$ at 25 and 34 bar ($CO/H_2/N_2$ =32/64/4, 34 bar). 60

Table 4.14. Yield of main products with HiFUEL R120-10 % $CeO_2/\ \delta\text{-}Al_2O_3$ at 25 and 34 bar ($CO/H_2/N_2$ =32/64/4, 34 bar). 60

Table 4.15. Yield of by-products with HiFUEL R120-10 % CeO_2/ δ-Al_2O_3 at 25 and 34 bar ($CO/H_2/N_2$ =32/64/4, 34 bar). 60

Table 4.16. Selectivity of main products with HiFUEL R120-5% CeO_2/δ-Al_2O_3 at different inlet H_2/CO ratios (300^oC, 34 bar) ……..…… 62

Table 4.17. Yield of main products with HiFUEL R120-5% CeO_2/δ-Al_2O_3 at different inlet H_2/CO ratios (300 ^oC, 34 bar). 62

Table 4.18. Yield of by-products with HiFUEL R120-5% CeO_2/δ-Al_2O_3 at different inlet H_2/CO ratios (300 ^oC, 34 bar). 62

Table 4.19. Selectivity of main products with HiFUEL R120-10% CeO_2/δ-Al_2O_3 at different inlet H_2/CO ratios (300^oC, 34 bar). ……..…… 65

Table 4.20. Yield of main products with HiFUEL R120-10% CeO_2/δ-Al_2O_3 at different inlet H_2/CO ratios (300 ^oC, 34 bar). 65

Table 4.21. Yield of by-products with HiFUEL R120-10% CeO_2/δ-Al_2O_3at different inlet H_2/CO ratios (300 ^oC, 34 bar). 65

LIST OF SYMBOLS

gcat	Catalyst weight in grams
h	Hour
NOx	Nitric oxides
n	Molar flow rate
ml	Milliliter
wt	Weight
ΔH_r°	Standard enthalpy of reaction

LIST OF ACRONYMS/ABBREVIATIONS

BET	Brunauer, Emmet and Teller
BPR	Back Pressure Regulator
BTRS	Bench Top Reactor Systems
CSTR	Continuous Stirred-Tank Reactor
DME	Dimethyl Ether
FTIR	Fourier Transform Infrared Spectroscopy
GC	Gas Chromatography
GCMS	Gas Chromatography-Mass Spectrometry
GHSV	Gas Hourly Space Velocity
GLS	Gas Liquid Separator
HMI	Human Machine Interface
MCM-41	Mobil Composition of Matter- 41
MFI	Mobil Five
LPG	Liquefied Petroleum Gases
PLC	Programmable Logic Controller
SEM	Scanning Electron Microscopy
TPR	Temperature-Programmed Reduction
XANES	X-Ray Adsorption Near Edge Structure
XPS	X-Ray Photoelectron Spectroscopy
XRD	X-Ray Diffraction
ZSM-5	Zeolite Socony Mobil-5

1. INTRODUCTION

Projections in energy demand are expected to be very high in the future particularly in the Pacific and Asian regions. In supplying safe energy with zero global warming and ozone depleting potential, dimethyl ether (DME) is considered as a promising clean fuel. DME (CH_3OCH_3), which is non-toxic and colorless, is the simplest ether that can be synthesized from carbon-based feeds. DME can be used as motor fuel replacing diesel and LPG, or as a high-performance coolant instead of chlorofluorocarbons. Furthermore, DME has very low NO_x and no SO_x emissions in addition to reduced particulate matter through its burning process; it also has a high cetane number of 55-60 and high oxygen content, which makes DME an attractive fuel additive or alternative fuel for a sustainable future [1–4].

DME synthesis can be carried out by indirect and direct methods. The indirect method includes three separate reactions, namely methanol synthesis, methanol dehydration and water-gas shift, whereas the direct method combines all these steps in a single reactor [5].

Bi-functional catalysts are generally used for better control over the reactions occurring spontaneously, and the catalysts commonly used are combinations of a methanol synthesis component with an acidic solid partner [6]. Recent studies have mainly focused on using Cu-Zn on Al_2O_3 for methanol synthesis and solid acid catalysts such as γ–Al_2O_3, zeolites, silica-alumina and SAPO for methanol dehydration [7].

In this study, the aim was to design catalyst systems with enhanced catalytic performance, selectivity and durability. For this reason, the commercial Cu-Zn based methanol synthesis catalyst (HiFUEL-R120) was coupled with CeO_2-loaded δ-Al_2O_3 catalyst prepared by the impregnation method. The CeO_2 loading on δ-Al_2O_3 is known to increase surface basicity, which is an undesired property for methanol dehydration;

however, it also shifts the water-gas shift reaction towards higher H_2 production, thus enhancing methanol synthesis [8].

In the parametric study, temperature, pressure, feed ratio and the level of CeO_2 loading were selected as the four experimental parameters to be tested for their effects on catalyst performance, which was expressed in terms of CO conversion along with DME, methane (CH_4), carbon dioxide (CO_2) and methanol (CH_3OH) yields and selectivity.

Chapter 2 surveys the literature on DME, its properties and synthesis methods, reactor types, and the catalysts used in recent studies for DME synthesis. The experimental study carried out in this work is explained in detail in Chapter 3, while the results obtained are presented, illustrated and discussed in Chapter 4. Chapter 5 includes the conclusions drawn from the experimental work as well as the recommendations for future studies.

2. LITERATURE SURVEY

2.1. Dimethyl Ether as an Alternative Fuel

Global warming and diminishing oil reserves to supply energy demand are the most crucial problems of the future. Higher levels of carbon dioxide in the atmosphere due to increasing usage of fossil fuels are the main reasons of global warming [9].

Fuels considered as alternative energy sources in the next century should have properties that make them usable as good replacements. Therefore, high performance, accessibility, renewability and easy storage and distribution are the main focuses for a new energy source. While many studies are focused on methane, hydrogen, methanol, Fischer-Tropsch fuels and bio-fuels, dimethyl ether (DME) stands out as one of the most promising alternative fuels [10].

2.2. Properties of Dimethyl Ether

Dimethyl ether has a chemical formula of CH_3OCH_3 and can be considered as the simplest ether (Figure 2.1). DME exists in the form of a liquefied gas at a pressure of 6 bar (or -24.9^oC @ 1 bar) and its usage infrastructure is similar to Liquefied Petroleum Gas (LPG). The cetane number of DME is 55-60, and it is therefore a great feedstock for providing improved engine performance in vehicles [10–12]. Dimethyl ether is non-carcinogenic, non-toxic, non-teratogenic and non-mutagenic unlike most other volatile organic compounds [11]. Characteristic properties of DME are compared with other alternative fuels in Table 2.1. and Table 2.2.

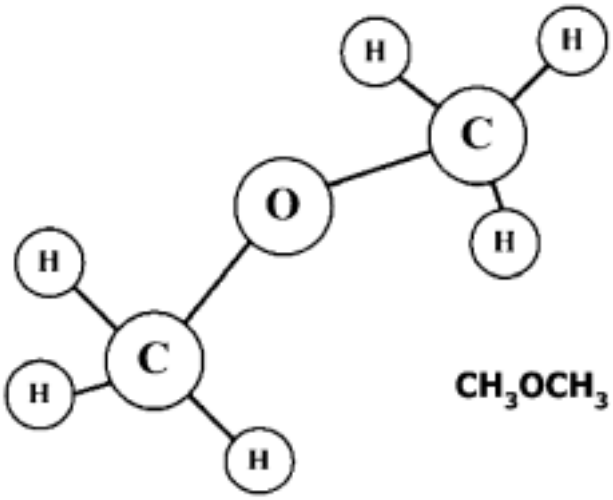

Figure 2.1. Structure of dimethyl ether [3].

DME provides excellent functioning in gas turbines due to its low emissions of CO, NO_x and unburned hydrocarbons. However, its high cetane number makes DME an unsuitable fuel source for spark-ignition (SI) engines although its other chemical properties are acceptable [3].

Table 2.1. Comparison of chemical and physical properties of DME with some commonly used fuels [10,11,13-15].

Properties	**DME**	**Methane**	**Methanol**	**Ethanol**	**Propane**	**Gasoline**	**Diesel**
Chemical formula	CH_3OCH_3	CH_4	CH_3OH	C_2H_5OH	C_3H_8	C_7H_{16}	$C_{14}H_{30}$
Molecular weight (g mol^{-1})	46.07	16.04	32.04	46.07	-	100.2	198.4
Boiling point (°C)	-24.9	-162	64	78	-42	38-204	125-400
Liquid density (g cm^{-3}) (@293 K)	0.661	0.00072	0.792	0.785	0.49	0.737	0.856
Specific gravity of gas (vs. air)	1.59	0.55	-	-	1.52	-	-
Heat of vaporization (kJ/kg)	467	1097	510	-	426	-	-
Vapor pressure (bar) (@293 K)	6.1	-	-	-	9.3	-	-
Ignition temperature (K)	623	905	743	-	777	-	-
Explosion limit	3.4-17	5-15	5.5-36	-	2.1-9.4	-	0.6-6.5
Cetane number	55-60	0	5	-	5	-	40-55
Net calorific value (10^6J/kg)	28.90	50.23	21.10	-	46.46	-	41.86
Carbon content (wt. %)	52.2	0.74	37.5	52.2	-	85.5	87

2.3. Environmental and Economic Impacts

The feedstock for the production of methanol, and hence DME, is synthesis gas which is not a natural resource; therefore, DME production is cost related. Generally natural gas is used as the starting resource to produce synthesis gas for subsequent methanol and DME production, and consequently, the price of the natural gas is influential. Use of renewable raw materials for syngas production is also being investigated to compensate for the rising natural gas prices [11].

2.4. Dimethyl Ether as Energy Carrier

Methanol and DME, which are environmental friendly clean fuels, and their production from carbon monoxide and carbon dioxide is an effective process to obtain a secondary energy carrier for renewable energy utilization [13].

2.5. Production of Dimethyl Ether

2.5.1. Indirect Synthesis Method

In the indirect method, DME is synthesized by a two-step process conducted separately; first, synthesis gas is reacted to form methanol, and then methanol is dehydrated to DME. The reaction for DME production through methanol dehydration is given in Eq 2.1:

$$2CH_3OH \leftrightarrow CH_3OCH_3 + H_2O \qquad (2.1)$$

Previous research indicates that methanol dehydration kinetics on solid catalysts can be described by kinetic models based on Langmuir-Hinshelwood or Eley-Rideal mechanisms, with water and DME acting as reaction inhibitors [7]. Furthermore, thermodynamics of methanol dehydration show that the exothermic reaction also gives some by-products such as ethylene, carbon monoxide, hydrogen and coke which are generally more important at higher temperatures.

A diagram of the general DME production process is given in Figure 2.2 [7].

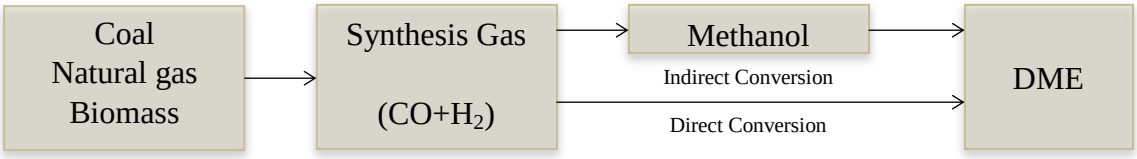

Figure 2.2. Process diagram for DME production [7].

2.5.2. Direct Synthesis Method

The direct synthesis of DME can be described mainly by two overall reactions, as given by Equation 2.2 and Equation 2.3. The overall reaction in Equation 2.2 involves three reaction steps in a single reactor over two independent bi-functional catalysts; firstly, methanol synthesis from syngas occurs as given in Equation 2.4 over the Cu-Zn based metallic catalyst, then *in situ* methanol dehydration to DME as specified in Equation 2.5 and the accompanying water-gas shift reaction of Equation 2.6 ensue over the acidic catalyst partner. In the absence of water-gas shift activity, the overall reaction given in Equation 2.3 is valid [14].

$3CO + 3H_2 \leftrightarrow CH_3OCH_3 + CO_2$	$\Delta H_r° = -246$ kJ/mol	(2.2)
$2CO + 4H_2 \leftrightarrow CH_3OCH_3 + H_2O$	$\Delta H_r° = -182$ kJ/mol	(2.3)
$CO + 2H_2 \leftrightarrow CH_3OH$	$\Delta H_r° = -90.7$ kJ/mol	(2.4)
$2CH_3OH \leftrightarrow CH_3OCH_3 + H_2O$	$\Delta H_r° = -23$ kJ/mol	(2.5)
$CO + H_2O \leftrightarrow CO_2 + H_2$	$\Delta H_r° = -41.2$ kJ/mol	(2.6)

DME production by direct synthesis increases overall catalytic performance of the reaction system resulting in CO conversion levels around 80%, while these remain at about 20% in indirect synthesis, which is explained by the argument that in the direct synthesis method, the surface concentration of the intermediate methanol is decreased readily which results in better thermodynamic conditions for higher CO conversion [15].

2.6. Types of DME Reactors

High energy efficiency is desired for the catalytic reactions involved in this reaction system, and therefore, the type of reactor used plays an important role. Fixed bed reactor types are generally used in pilot scale DME synthesis; however, slurry phase reactors and fluidized-bed reactors are also highly suggested for these studies [7].

Fixed bed reactors are better in avoiding problems related to loss of fine catalyst particles and scale-up; however, there is the difficulty of the development and/or existence of hot spots in fixed bed reactors. Thus, catalyst deactivation should be avoided at certain temperatures under feasible conditions. Numerical simulation are conducted to show that reactor temperature can be taken under control by avoiding high heats of reaction and large temperature differences by designs allowing high heat transfer coefficients and large heat exchange areas [16].

Fluidized bed reactors are suggested for DME synthesis as compared with slurry or fixed bed reactors due to the fact that the former provide high mass and heat transfer efficiencies. However, although it was shown that DME selectivity and catalytic activities are higher in fluidized beds than in slurry or fixed bed reactors, their feasibility and scale-up efficiencies have not been developed yet [17].

2.7. Catalysts Used for DME Synthesis

2.7.1. Methanol Synthesis Catalysts

Takeguchi *et al.* (2000) studied different hybrid catalysts for dimethyl ether synthesis from syngas. In this research, methanol-synthesis catalysts (MSC) and methanol dehydration silica alumina catalyst (SA) were prepared by the uniform-gelation method, and mechanochemical activation of mixtures of the silica gel and the $Al(OH)_3$ precursor, respectively. Mixing of these catalysts was achieved by two different methods, in one method the catalysts were milled, tableted and pulverized together, and in the

second method the catalysts were tableted and pulverized separately and then mixed together. Activity tests were run in a high-pressure fixed bed flow reactor at a moderately low temperature (230 °C) at 70 bar. Catalyst characterization tests were conducted to observe the effects of water on acid properties of the catalyst and on the overall reaction. It is claimed that when pressure is increased above atmospheric, water produced by methanol dehydration and adsorbed on Lewis acid–base pairs of the surface becomes an inhibiting factor that decreases DME formation; these pairs were formerly the major active sites for methanol dehydration at atmospheric pressure. The catalyst system that was least affected by this occurrence and the most effective was the methanol synthesis ($CuO/ZnO/Ga_2O_3$) catalyst coupled with silica-alumina catalysts, which showed a high dimethyl ether (DME) yield of 55.5% with a good selectivity of 93.5% [18].

Lima *et.al.* (2014) investigated the effect of niobia (Nb_2O_5) promotion over conventional $CuO\text{-}ZnO\text{-}Al_2O_3$ on direct synthesis of DME. The catalytic activity was tested at 265 °C and 5 MPa (ca. 49 bar) in a liquid-phase CSTR, using n-hexadecane as the catalyst suspension medium. Niobia promotion over alumina gave higher catalytic activity than pure alumina, and the highest catalytic activity was obtained with the lowest niobia addition to alumina (5.9 wt.% Nb_2O_5). Since surface acidity plays an important role on the methanol dehydration activity of the catalyst it was found that the addition of niobia led to lower surface basicity on alumina, and hence, the tolerance of methanol dehydration catalysts to the CO and CO_2 present in the medium was increased [19].

Unlike conventional $Cu\text{-}Zn\text{-}Al_2O_3$ (also termed as CZA) catalysts, the performances of Cu–Mn–Zn catalyst coupled with La, Ce, Pr, Nd, Sm and Eu modified-Y catalysts were also investigated in DME direct synthesis by Jin *et al.* (2007). Cu–Mn–Zn was prepared by co-precipitation and modified-Y catalysts were prepared by ion exchange and bi-functional catalysts were mechanically mixed. Reaction tests were carried out in fixed bed reactor at 20 bar and 245 ^{o}C. Investigations showed that Cu–Mn–Zn/La–Y and Cu–Mn–Zn/Ce–Y were more active than Cu–Mn–Zn/pure-HY. Furthermore, the maximum CO conversion achieved was 77.1% and DME selectivity was 66.6% on Cu–Mn–Zn/Ce–HY. The high stability of the Ce-modified zeolite Y in

DME synthesis was found to result from the high proportion of moderate-strength acid sites on the catalyst [20].

2.7.2. Methanol Dehydration Catalysts

The research activities for methanol dehydration have focused on acidic solid types such as Al_2O_3, silica-alumina (SiO_2-Al_2O_3) and zeolites such as HY, HZSM-5 and HMCM-49, meso-porous materials (MCM and SAPO families), or ZrO_2 [21,22].

At present, most studies on methanol synthesis from syngas, and also its commercial production, are normally run on traditional CuO-ZnO-Al_2O_3 (CZA) catalysts. Methanol dehydration is carried out mostly over γ-Al_2O_3 [23–27]. In the latter, pore size distribution and acidic-site strength affect mainly catalytic activity and selectivity. Although there is a direct relationship between the activity of a methanol dehydration catalyst and its surface acidity, high acidity is not a desired property since it causes further conversion of DME to hydrocarbons. Thus optimum acidity is a crucial property for having higher conversion and selectivity [28].

Ramos *et al.* (2005) investigated the effect of dehydration acid catalyst features on direct DME synthesis. In this study, methanol synthesis and methanol dehydration catalysts (Al_2O_3, HZSM-5, W-ZrO_2 and sulfated-ZrO_2) were used in high-pressure reactor units. Catalyst characterization tests showed that activity of acidic solids in DME synthesis was determined by the amount sites with high acidity and their acid strength. Addition of acid to the catalyst improved CO conversion because of the more intensely initiated methanol synthesis reaction. As a result, HZSM-5 found to be the most effective among other catalyst by giving the highest DME selectivity [29].

In their study, Kang *et al.* (2008) examined biomass based synthesis gas conversion to DME using the direct synthesis method with Cu/ZnO/Al_2O_3 (CZA) methanol synthesis catalyst. The CZA catalyst (46:40:14, w/w/w/w) and the methanol dehydration catalysts such as Zr modified proton-type zeolites including ferrierite (Si/Al = 25), ZSM-5 (Si/Al = 50) and Y (Si/Al = 2.3) were prepared by wet impregnation and co-precipitation, respectively. Reaction tests were conducted in a tubular fixed bed reactor at 250°C and

40 bar, it was reported that CZA coupled with the Zr-modified ferrierite catalyst gave the highest CO conversion of 49.0% and DME selectivity of 58.2%. The reason why DME synthesis was highly promising is that the overall activity of the catalyst system for direct DME synthesis depends on BET surface area and surface acidity, which was achieved with the composite CZA catalyst coupled with Zr-modified ferrierite. Nevertheless, DME synthesis was supported more strongly by methanol dehydration over acid sites rather than by methanol formation over metallic sites [30].

Xu *et al.* (2008) studied the influence of using CaO modified H-ZSM-5 (Si/Al=38) methanol dehydration catalyst prepared by the equal-volume method together with the conventional methanol synthesis catalyst (JC207, Jingjing Catalyst Plant, China) on the catalytic activity in a fixed bed tubular reactor. As also shown in other studies, it was concluded that good distribution of acidic sites is crucial for achieving high catalyst activity. A decrease was observed in DME selectivity at CaO loadings above 3wt%, showing restricted synergy and uneven distribution of acidic sites for DME formation, which was proposed to be caused by the transformation of Brönsted acid sites into Lewis acid sites [31].

Cai *et al.* (2015) observed the effect of tin promotion on the DME synthesis performance of the bi-functional Cu-Zn-Al/HZSM-5 catalyst at 260^{o}C and 20 bar. The CuO–ZnO–Al_2O_3, xSn-CZA, HZSM-5 and hybrid catalysts were prepared by co-precipitation, incipient-to-wetness impregnation and calcination of NH_4-ZSM5, respectively. Catalyst samples were characterized by H_2-TPR, XPS, in-situ XRD, in-situ XANES and FTIR analyses. It was observed that the presence of Sn in reduced state modifies the electronic state of Cu, and hence it was proposed that if selective deactivation of positively charged Cu sites active in WGS can be accomplished, then the selectivity of DME may be enhanced since methanol synthesis and WGS are affected by different active species. WGS reaction was suppressed by Sn addition, resulting in less CO_2 generation and higher DME selectivity but lower CO conversion. The optimum amount of Sn that did not decrease CO conversion was 0.1 wt. %, methanol and DME selectivity were slightly increased. Maximum CO conversion and DME selectivity were found as 19.1% and 76.1%, respectively [32].

Lee *et al.* (2014) suggested that DME selectivity indirect synthesis can be improved by concealing strong acid sites especially on zeolite type catalysts. In this research, Al_2O_3 modification of acid sites on H-ferrierite was studied. Co-precipitation method was used to prepare bi-functional CuO–ZnO–Al_2O_3 catalysts deposited on Al_2O_3-modified H-ferrierite. A fixed bed tubular reactor at 250 °C and 3.5 MPa (ca. 34 bar) and was used to run the reactions at a space velocity of 2000 ml/gcat.h. Higher dispersion of CuO–ZnO–Al_2O_3 on H-ferrierite proved to be one of the major reasons for enhanced DME selectivity and CO conversion. Catalyst characterization tests established high interaction of copper particles and development of small copper particles around the optimum 2.5-5 wt. % Al_2O_3 loading on H-ferrierite. Al_2O_3 deposition on H-ferrierite was found to reduce the number of strong acid sites, increase the dispersion of copper particles and decrease byproduct formation [33].

Song *et al.* (2014) studied the role of ZrO_2 promotion in direct DME synthesis. Bi-functional Cu-ZnO-Al_2O_3-ZrO_2 (x)/γ-Al_2O_3 catalyst was prepared by co-precipitation. Reaction tests were conducted in a continuous-flow reactor at 270 °C, 5 MPa (ca. 49 bar), a GHSV of 1500 h^{-1}, and a feed composition (H_2/CO/CO_2/CH_4) by volume of 52/24/23/1, respectively. Combining the results of catalyst characterization and activity tests, it was concluded that higher Cu surface area achieved by higher metal dispersion enhances both CO conversion and DME selectivity which is the slowest step of series reactions. Moreover, maximum CO and CO_2 conversions are obtained with a Zr loading of 3 mol% [34].

Migliori *et al.* (2014) investigated the effect of Si/Al ratio of H-MFI catalysts on the kinetic parameters of methanol dehydration reaction in the methanol-to-DME process. Reaction tests were performed at 230 °C and 250 °C and atmospheric pressure. It was confirmed that catalyst performance is enhanced by higher catalyst acidity, lower Si/Al ratios require higher activation energy for the dehydration reaction, and decreasing the Al content of the Si/Al ratio increases the Si/Al ratio, but the discrepancy between the Si/Al ratios in the gel and in the zeolite increases [35].

Jiang *et al.* (2004) prepared H-ZSM-5 and NaH-ZSM-5 zeolites for methanol dehydration in the DME synthesis process. The results were compared with commercial γ-Al_2O_3 and it was concluded that H-ZSM-5 and NaH-ZSM-5 zeolites show higher catalytic activity. This result was explained by the Brönsted and Lewis acid sites on these zeolites. As acidity can be arranged by adjusting the Si/Al ratio, catalytic activity increased while DME selectivity decreased at lower Si/Al ratios. Furthermore, due to removal of strong acid sites Na^+ ion exchanged H-ZSM-5 showed higher DME selectivity [36].

Wang *et al.* (2014) synthesized DME from syngas over CuO-ZnO-Al_2O_3@SiO_2-Al_2O_3 core-shell structure catalyst prepared by facile hydrothermal treatment. The core–shell catalyst was synthesized using tetraethylorthosilicate, silica sol, or water glass as the silica source, aluminum nitrate as the aluminum source, and without using any aid, alkali or amine template to avoid etching of core material, CuO–ZnO–Al_2O_3; the shell material was amorphous SiO_2-Al_2O_3. Syngas with H_2/CO molar ratio of 2 was reacted at 220-320 °C and 2-6 MPa (ca. 20-60 bar) with a GHSV of 1000-4000 ml/gcat.h. Comparison with the CZA catalyst showed the increase achieved in CO conversion from 18.9% to 55.7-71.1%. Since acidity plays an important role in catalytic activity, shell thickness and acidity was changed by hydrothermal treatment. The core–shell catalyst with Si/Al ratio of 1/3 exhibited the highest CO conversion of 71.1% with a DME selectivity of 61.9% owing to its relatively higher acid strength and suitable shell thickness [37].

Matsumura *et al.* (2001) used CeO_2-supported ultrafine Pd particles in low-temperature methanol synthesis. The catalysts were prepared by co-precipitation, and the reaction was carried out in a fixed bed reactor continuous reactor at 170-200 °C and 0.1-3.0 MPa (1-30 bar). It was found that pre-reduction temperature has influence on the methanol yield since catalysts pre-reduced at 300 °C gave higher methanol yields than those pre-reduced at 500 °C. Moreover, the maximum methanol yield of over 15% was obtained at 170 °C and 3.0 MPa over 15 wt. %Pd/CeO_2 pre-reduced at 300 °C [38].

Imamura *et al.* (1999) examined the effect of CeO_2 on Pd/Al_2O_3 in the syngas-to-DME process. Pd/MgO, Pd/ZrO_2, Pd/SiO_2 and Pd/TiO_2 were also prepared for comparison; the results showed that addition of CeO_2 increased CO conversion from 2.4% to 9.4% and also the DME selectivity to 79%. This was explained by the importance of acid sites in getting higher yields of DME. Since Al_2O_3 has higher acidity, the best results were obtained on $Pd/CeO_2/Al_2O_3$. Investigation of the surface structure of $Pd/CeO_2/Al_2O_3$ clearly showed that the addition of CeO_2 increases the dispersion of Pd [39].

Xie *et al.* (2015) investigated the influence of different zeolites on the catalytic activity for methanol dehydration in the single step synthesis of DME from syngas. Co-precipitation was used for the preparation of precursor $CuO\text{-}ZnO\text{-}Al_2O_3$, and as a solid acid component, four commercial zeolite types (H-ZSM-5, H-Y, H-Beta, and H-Ferrierite) were purchased. Reactions were carried out at 260 °C and 50 bar. In the direct DME synthesis method, methanol dehydration is directly related with large amount of weak acid sites on the surface which is the major reason for achieving higher DME selectivity with CZA/ZSM-5, CZA/Y and CZA/Ferrierite. The highest CO conversion achieved on CZA-Y was 91.9% [40].

Montesano *et al.* (2014) studied shape-selectivity in $Cu/ZnO/Al_2O_3$ and zeolite catalysts (Theta-1, ZSM-23, ferrierite, ZSM-5 and mordenite) in the syngas-to-DME conversion process. Catalytic activity tests were performed in continuous-flow micro-reactors at 250-270 ^oC and 30 bar. It was found that Theta-1 and ferrierite catalysts provide the most stable performance and the highest selectivity to DME. Having larger crystallite sizes which lead to the formation of less volatile species, ZSM-23 showed lower stability amongst other zeolites. Furthermore, deactivation and higher selectivity to hydrocarbons are results of bulky species within the pores and channel intersections of zeolites like mordenite and ZSM-5 [41].

Fei *et al.* (2006) studied methanol dehydration to produce DME and used HY zeolite and Fe-, Co-, Ni-, Cr-, or Zr-modified HY zeolite for methanol dehydration as well as modified HY zeolite-supported Cu–Mn–Zn catalysts for direct synthesis of DME

from syngas. Cu–Mn–Zn was prepared by the conventional co-precipitation method and then physically mixed with HY zeolite modified via ion-exchange. Reactions were conducted in a high-pressure micro-reactor system at 20 bar and 245 °C. For methanol dehydration it was found that HY zeolites modified with Zr- and Ni- provided higher catalytic activity and stability, while the Fe-, Co-, and Cr-modified HY zeolites showed lower CO conversion, mainly owing to carbon deposition [42].

Yoo *et al.* (2007) used SAPO-34, -18, -11, and -5 as methanol dehydration catalysts in DME synthesis together with the conventional CZA as the methanol synthesis catalyst. Catalysts were prepared by the gel solution method, and catalytic tests were carried out in fixed bed reactors at 42 bar and 260 °C. SAPO-34 and SAPO-18 were found to have strong acid sites and showed high initial activity, yet quick deactivation ensued due to pore blockage. However, SAPO-5 and SAPO-11 showed significant catalytic stability and activity [43].

2.8. Catalyst Preparation Methods

Moradi *et al*. (2007) focused their research on the impact of hybrid catalyst preparation methods on direct synthesis of DME from synthesis gas. Seven different preparation methods were compared: co-precipitation with Na_2CO_3 and $NaAlO_2$, co-precipitation impregnation, co-precipitation sedimentation, sol-gel and novel sol-gel impregnation techniques. Reactions were tested in a micro slurry reactor at 240 °C and 40 bar. The most effective catalyst was the one prepared by a novel sol-gel impregnation method due to the highly dispersed Cu on its structure, and the optimum weight ratio for $CuO/ZnO/Al_2O_3$ was found as 2:5:1 [44].

Ahmad *et al.* (2014) investigated the effect of catalyst preparation methods on catalyst activity and attributes such as CO conversion and DME selectivity. In their study, co-precipitation–impregnation, impregnation, co-precipitation sedimentation and oxalate co-precipitation was applied for the preparation of various catalyst types. Five bi-functional catalysts (CZA-Z-CF, CZA-Z-IP, CZA-Z-CS, CZA-Z-OX) were used in

addition to an admixed catalyst system (CZA-Z) used as reference. CuO-ZnO-Al_2O_3 functioned as a precursor in varying amounts in all catalysts; the reaction was conducted in a fixed bed reactor located in a continuously operating laboratory set-up. Catalysts prepared by co-precipitation-impregnation and impregnation methods showed low activity due to their low metal dispersion and large crystallite sizes. In contrast, those synthesized with the co-precipitation sedimentation and oxalate co-precipitation methods gave more favorable results, especially the catalyst prepared by oxalate co-precipitation gave both high DME selectivity and high CO conversion. Furthermore, size of Cu surface areas and particles and number of adequate acidic sites played an important role in optimum catalytic activity [45].

Khoshbin and Haghighi (2014) studied the influence of preparation method and active phase on CO conversion in the direct syngas-to-DME (STD) process. Nano-catalysts comprising CZA ($CuO–ZnO–Al_2O_3$) as active phase and HZSM-5 as support were prepared by utilizing a hybrid co-precipitation-ultrasound method. Catalytic properties were tested in a fixed bed micro-reactor operated at 200-300^oC, 10-40 bar, a GSHV of 600-1500 $cm^3g^{-1}h^{-1}$ and a H_2/CO molar ratio of 2. Surface morphology tests exhibited direct dependency between the average size distribution of nano-catalysts and the increasing $CuO–ZnO–Al_2O_3$/HZSM-5 ratio, which is caused by the aggregation of CZA particles. However, this ratio does not have a particular effect on surface area according to BET results. Operating conditions were also investigated by adjusting reaction temperature, pressure, GHSV at different active phase ratios. The results were found to be reliable since they are consistent with other studies. Optimum reaction temperature and pressure were chosen as 275 °C and 40 bar, respectively [46].

In their report, Phienluphon *et al.* (2015) used a different and basic method called physical coating (PhyC) for the preparation of a zeolite shell catalyst without using a hydrothermal synthesis process. As the core catalyst Cu/ZnO/Al_2O_3 (CuZnAl) and as the shell PhyC-prepared silicoaluminophosphate-11 (SAPO-11) were used and brought together as CuZnAl/SAPO11-PhyC. CZA catalyst was prepared by co-precipitation and the zeolite capsule catalyst was prepared by physical coating (PhyC) method. Catalytic activities were measured in a fixed bed reactor at 50 bar and 250^oC.As a result, CO

conversion and DME selectivity were found as 92.0% and 90%, respectively [47].

Martinez *et al.* (2012) studied physically mixed hybrid CuZnAl (CZA)/HZSM-5 catalysts and their effect on methanol dehydration reaction. The following procedure is used in the mixing method: grinding of powders prior to pelletizing (grinding method), slurrying the two solids in water followed by drying and pelletizing (slurry method), and physical mixture of pre-pelletized components. Experimental results showed that the decrease in Brønsted acidity led to a decrease in the activity of the zeolite which gave rise to much lower efficiency of the corresponding hybrids for DME synthesis at typical STD conditions, in comparison to the catalyst prepared by simple mixture of pre-pelletized components. Moreover, relatively lower CO conversions and DME yields were obtained with catalysts prepared by grinding and slurry methods in comparison with the catalyst utilized by the mixing of individual pellets, for which no interactions between components are expected to occur [48].

In their study, Khoshbin and Haghighi (2013) examined the effect of preparation method on catalytic activity and DME selectivity in the direct syngas-to-DME method. Impregnation, co-precipitation-physical mixing and combined co-precipitation-ultrasound methods were used to prepare CuO-ZnO-Al_2O_3/HZSM-5 nano-catalysts. The results indicated that CO conversion reached 50% at 275 °C and 40 bar on the catalyst prepared by co-precipitation-ultrasound. At higher temperatures, all catalysts showed lower catalytic activity, which was explained by the thermodynamic restrictions on exothermic reactions [49].

Li *et al.* (2014) studied the effect of preparation method for Cu-La_2O_3-ZrO_2 /γ-Al_2O_3 hybrid catalysts on CO hydrogenation to DME. As the number of acidic sites plays an important role in DME selectivity, they examined the surface acidity levels and found that CLZ-A-S, which was prepared by the stirring of precursors of CLZ and γ-Al_2O_3 and calcination at 500 °C, has the highest surface acidity and hence the highest DME yield, selectivity and CO conversion of 58%, 80% and 73%, respectively [50].

Nie *et al.* (2012) studied a series of core–shell structured CuO–ZnO@H-ZSM-5 (CZ@H) catalysts which were prepared by homogeneous precipitation through urea hydrolysis. Reaction tests were carried out in a fixed bed reactor at 20 bar and 260 ^{o}C with a GHSV of 1500 ml/gcat.h. It was suggested that this preparation method provided a well-defined catalyst structure, high contact area between the methanol synthesis sites and methanol dehydration sites and created high Cu dispersion. Therefore both high CO conversion and high DME selectivity were achieved as 91.8% and 71.4%, respectively [51].

2.9. Factors Affecting the Activity of DME Synthesis Catalysts

2.9.1. Water Content

Production of water by the reverse water-gas shift reaction may affect DME selectivity at higher reaction temperatures by inhibiting methanol dehydration by shifting this reaction backward. Furthermore, water may also block and hydrate through the pores of the solid acid catalysts such as γ-Al_2O_3, thus catalytic activity is decreased owing to the hydrophilic property of water [52].

Water may have a positive effect on the catalysts, on the other hand, by regenerating the catalyst if carbon formation is likely. However, processing with certain catalysts such as H-MOR do not require an additional step for water removal or addition since the catalyst has large pore size providing enough space for complete coking [53].

2.9.2. H_2/CO Molar Ratio

The effect of feed composition is accepted to have a great influence on catalytic activities. H_2/CO molar ratio is found to be optimum when it is 1 or 1.5. However, since methanol dehydration and methanol synthesis occur spontaneously in the direct synthesis method, a degree of trade-off in feed gas compositions may be required. Methanol synthesis reaction runs faster in H_2-rich medium whereas methanol dehydration does better in a CO-rich medium to provide enough water for the water-gas shift reaction [54].

Furthermore, H_2/CO ratios may also be selected so as to lower coke deposition on certain catalysts. Therefore, the H_2/CO ratio must be must be optimized for each reaction system [16,17] .

2.9.2. Operating Conditions

Recently, Huang *et al.* (2015) studied effects of physically mixed catalysts, temperature of the reaction and H_2/CO molar ratio on DME hydrogenation while keeping space velocity at 15,000 ml/gcat.h. For syngas to methanol process, Cu-ZnO-$Al_2O_3$and Pd-Cu-ZnO-Al_2O_3 catalysts were prepared by co-precipitation and impregnation, respectively. Furthermore, no hysteresis effect observed in the course of varying the reaction temperature, which proved that catalyst performance was stable and reversible. When H_2/CO molar ratio was set at 1, maximum DME space-time yield was achieved as 2.3 g/gcat.h. Effect of dehydration catalyst (i.e., γ-Al_2O_3, ferrierite, or HZSM-5) was also investigated and results depict that highest DME selectivity is achieved with γ-Al_2O_3while HZSM-5 generates the highest DME yield among other catalysts [55].

Ereña *et al.* (2005) examined the effect of operating conditions on the catalytic activity, selectivity and yields in CO/CO_2 hydrogenation to DME. CuO-ZnO-Al_2O_3/NaHZSM-5 was used for the parametric study carried out at operating conditions of 175–350 °C, and 10-50 bar. Temperature variations were found to be directly related with CO conversion and DME selectivity up to 275 °C where maximum conversion and DME selectivity were achieved around 85% and 50%, respectively [56].

Table 2.2. Production conditions in various studies on DME synthesis.

No #	Catalyst	Catalyst Preparation Method	Reactor Type	Pressure (bar)	Temperature (^{o}C)	Operating conditions	CO Conversion (%)	DME Selectivity (%)	References
1	CZA: Cr_2O_3: Ga_2O_3/Silica-Alumina	Uniform-gelation method	Fixed bed reactor	50-80	230–310	SV 4200-37600 h^{-1}	55.5	93.6	[18]
2	Niobia-modified CZA	Incipient to wetness impregnation	CSTR	50	264.85	-	9	64.9	[19]
3	Cu-Mn-Zn/Ce-HY- Cu-Mn-Zn/La-HY	Co-precipitation, Ion-exchange, mechanical mixing	Fixed bed reactor	20	245	SV=1500 h^{-1} H_2/CO=1.5	77.1, 76.7	66.7, 66.6	[20]
4	CZA-Y, CZA-ZSM5,CZA-Ferrierite	Wet-impregnation, Zr pretreatment, co-precipitation	Fixed bed reactor	40	250	SV = 5550 ($ml/g_{cat}.h$)	49	58.2	[30]

Table 2.2. Production conditions in various studies on DME synthesis (cont.).

No #	Catalyst	Catalyst Preparation Method	Reactor Type	Pressure (bar)	Temperature (^oC)	Operating conditions	CO Conversion (%)	DME Selectivity (%)	References
5	Tin-promoted CZA/HZSM-5	Sequential impregnation using incipient - to-wetness method	Fixed bed reactor	20	260	GHSV= (3600 (ml/gcat.h)	19.1	76.1	[32]
6	CZA/Al_2O_3-Ferrierite	Co-precipitation	Fixed bed tubular reactor	35	250	SV = 2000 (ml/gcat.h)	62.1	91.5	[33]
7	CZA-ZrO_2/γ-Al_2O_3	Co-precipitation	Fixed bed reactor	50	270	GSHV= 1500 (h^{-1})	79.3	85.8	[34]
8	CZA@SiO_2–Al_2O_3	Hydrothermal synthesis method	Fixed bed reactor	20-60	220–320	GHSV= 1000–4000 (ml/gcat.h)	71.1	61.9	[37]

Table 2.2. Production conditions in various studies on DME synthesis (cont.).

No #	Catalyst	Catalyst Preparation Method	Reactor Type	Pressure (bar)	Temperature (^oC)	Operating conditions	CO Conversion (%)	DME Selectivity (%)	References
9	CZA-Y, CZA/Ferrierite	Co-precipitation/physical mixing	Fixed bed reactor	50	260	GHSV= 1500 (ml/gcat.h)	91.9, 93	63.9, 61.4	[40]
10	HiFUEL R120, Theta-1, ZSM-23, ferrierite, ZSM-5 and mordenite	-	Micro flow continuous reactor system	30	270	SV = 8400 h^{-1}	14	60	[41]
11	Cu-Mn-Zn/Zr-HY(25 wt.% Zr-HY)	Co-precipitation/ ion-exchange/ mechanical mixing	High-pressure micro-reactor system	20	245	SV= 1500 h^{-1} $H_2/CO=1.5$	71.4	67.5	[42]

Table 2.2. Production conditions in various studies on DME synthesis (cont.).

No #	Catalyst	Catalyst Preparation Method	Reactor Type	Pressure (bar)	Temperature (^oC)	Operating conditions	CO Conversion (%)	DME Selectivity (%)	References
12	CZA/γ-Al_2O_3	Sol-gel impregnation	Micro slurry reactor	40	240	GHSV= 1000 (ml/gcat.h)	40.9	67.4	[44]
13	CZA-Z (zeolite H-MFI 400), CZA-Z-OX	Co-precipitation, oxalate co-precipitation	Fixed bed reactor	-	-	WHSV= 4.19 h^{-1}	69, 66	48, 45	[45]
14	CZA/HZSM-5 (nano-catalyst)	Co-precipitation, ultrasound	Fixed micro-reactor	40	275	GHSV= 600 (cm^3/g.h) H_2/CO=2	50	57	[46]

Table 2.2. Production conditions in various studies on DME synthesis (cont.).

No #	Catalyst	Catalyst Preparation Method	Reactor Type	Pressure (bar)	Temperature (^oC)	Operating conditions	CO Conversion (%)	DME Selectivity (%)	References
15	CZA/SAPO11-PhyC	Hydrothermal synthesis, co-precipitation, physical coating hydrothermal synthesis	Fixed bed reactor	50	250	-	92.0	90	[47]
16	CZA/HZSM-5	Hybrid co-precipitation–ultrasound	Micro-reactor	10-40	200-300	GSHV= 600 -1500 (cm^3gh^{-1})	50.5	55	[49]
17	Cu-La_2O_3-ZrO_2/γ-Al_2O_3 hybrid catalysts	Co-precipitation	Fixed bed reactor	40	260	GHSV= 1500 h^{-1}	73	58	[50]

Table 2.2. Production conditions in various studies on DME synthesis (cont.).

No #	Catalyst	Catalyst Preparation Method	Reactor Type	Pressure (bar)	Temperature (^{o}C)	Operating conditions	CO Conversion (%)	DME Selectivity (%)	References
18	CuO/ZnO/H-ZSM-5	Core-shell structured (H-ZSM-5 zeolite core enwrapped by one layer of a CuO–ZnO shell)	Fixed bed reactor	20	260	GHSV= 1500 (ml/gcat.h)	91.8	71.4	[51]
19	CZA and Pd/Cu/ZnO/Al$_2$O$_3$/γ-Al$_2$O$_3$, ferrierite, HZSM-5).	Co-precipitation	Fixed bed reactor	40	220	SV=15,000 (ml/gcat.h)	63	59	[55]
20	CZA/ NaHZSM-5	Co-precipitation	Fixed bed reactor	175-350	10-50	SV= 33.3 (gcat) h/mol	35	75	[56]

Table 2.2. Production conditions in various studies on DME synthesis (cont.).

No #	Catalyst	Catalyst Preparation Method	Reactor Type	Pressure (bar)	Temperature (^{o}C)	Operating conditions	CO Conversion (%)	DME Selectivity (%)	References
21	MgO modified HZSM-5	Dry impregnation method	Fixed bed reactor	40	260	GHSV= 1500 (ml/gcat.h)	96.3	64.5	[57]
22	CZA-SAPO	Gel solution-physical mixing	Fixed bed reactor	42	260	GHSV =6000 (ml/gcat.h)	58	45	[58]
23	CaO/HZSM -5	Impregnation	Fixed bed reactor	30	240-280	SV= 1300 (l/gcat.h)	75	78	[59]

3. EXPERIMENTAL WORK

3.1. Materials

3.1.1. Chemicals

Table 3.1 illustrates the chemicals used for the preparation of catalysts.

Table 3.1. Chemicals used for catalyst preparation.

Chemicals	Formula	Source	Molecular weight (g/mol)
Gamma Alumina	$\gamma -Al_2O_3$	Alfa Aesar	101.96
HiFUEL R120	Copper based methanol reforming catalyst	Alfa Aesar	-
Cerium (III) nitrate hexahydrate	$Ce(NO_3)_3 \cdot 6H_2O$	Sigma Aldrich	434.22

3.1.2. Gases and Liquids

Applications and specifications of the liquids and gases are listed in Table 3.2 and Table 3.3, respectively.

Table 3.2. Applications and specifications of the liquids used.

Liquid	Specification	Application
Water	Deionized (DI)	Aqueous solution

Table 3.3. Applications and specifications of the gases used.

Gas	Specification (%)	Supplier	Application
Helium	99.998	Linde	GC/MS Carrier Gas
Argon	99.995	Linde	GC Carrier Gas
Carbon monoxide	99.999	Hatgrup	Reactant
Hydrogen	99.995	Linde	Reactant, Reducing Agent
Nitrogen	99.998	Linde	Inert make-up gas used in reactions
Carbon dioxide	99.995	Linde	Product, GC calibration
Methane	99.995	Linde	Product, GC calibration
Dry Air	78.4% N_2+21.5% O_2	Linde	Automated pneumatic valve operation

3.2. Experimental Systems

Details of the experimental systems used in this study, i.e. catalyst preparation and testing systems and product analysis systems, are explained in the following sections.

3.2.1. Catalyst Preparation System

As mentioned in Section 2.4, DME synthesis involves both methanol synthesis and methanol dehydration. Therefore; use of a bi-functional catalyst approach is followed through the study. Commercial Cu-Zn based HiFUEL R120 catalyst, synthesized by Johnson-Matthey, and is used as the methanol synthesis catalyst. The catalysts, all of

which are prepared by incipient-to-wetness impregnation method, for methanol dehydration are listed as follows:

- 5% $CeO_2/\delta\text{-}Al_2O_3$
- 10% $CeO_2/\delta\text{-}Al_2O_3$
- 20% $CeO_2/\delta\text{-}Al_2O_3$

Preparation of the catalysts started with pretreatment of the $\gamma\text{-}Al_2O_3$. $\gamma\text{-}Al_2O_3$ is a commonly used methanol dehydration catalyst due to its high surface area. However, modification on $\gamma\text{-}Al_2O_3$ is necessary to increase its thermal stability. For this purpose, $\gamma\text{-}Al_2O_3$ is heat treated at 200 for 2h and then 900 °Cfor 4h to be transformed into $\delta\text{-}Al_2O_3$, which offers desired thermal stability at the expense of an acceptable decrease in total surface area down to ca. 81.6 m^2/g [60]. After this step, incipient-to-wetness impregnation method was applied to prepare ceria-modified alumina catalyst. In this method, a certain amount of alumina is kept under the vacuum in the vacuum Erlenmeyer flask in the ultrasonic mixer for 30 min. The aim of this step is to have homogenously mixed and open the pores of the support. The calculated amount of aqueous solution of $Ce(NO_3)_3 \cdot 6H_2O$ is dissolved in deionized water to obtain the desired CeO2 composition in the resulting catalyst. The amount of $\delta\text{-}Al_2O_3$ placed into the vacuum flask is determined such that 1.1 ml solution is contacted with 1 g of $\delta\text{-}Al_2O_3$ used. Aqueous $Ce(NO_3)_3 \cdot 6H_2O$ solution is then impregnated on to the alumina support in the vacuum flask at a rate flow rate of 0.5 ml/min^{-1} via silicone tubing using a Masterflex computerized-drive peristaltic pump. While feeding the $Ce(NO_3)_3 \cdot 6H_2O$ solution into the vacuum flask, the slurry is mixed ultrasonically to preserve the uniform penetration of the solution into the pores of $\delta\text{-}Al_2O_3$. After the impregnation process is completed, ultrasonic mixing is continued for an additional period of 90 min. Finally the resulting slurry is kept under overnight drying at 120 °C and then calcined under air environment at 325 °C for 4h. The schematic diagram of the incipient to wetness impregnation is illustrated in Figure 3.1. The steps of the preparation and pre-treatment of the ceria-modified $\delta\text{-}Al_2O_3$ is given in the Figure 3.1.

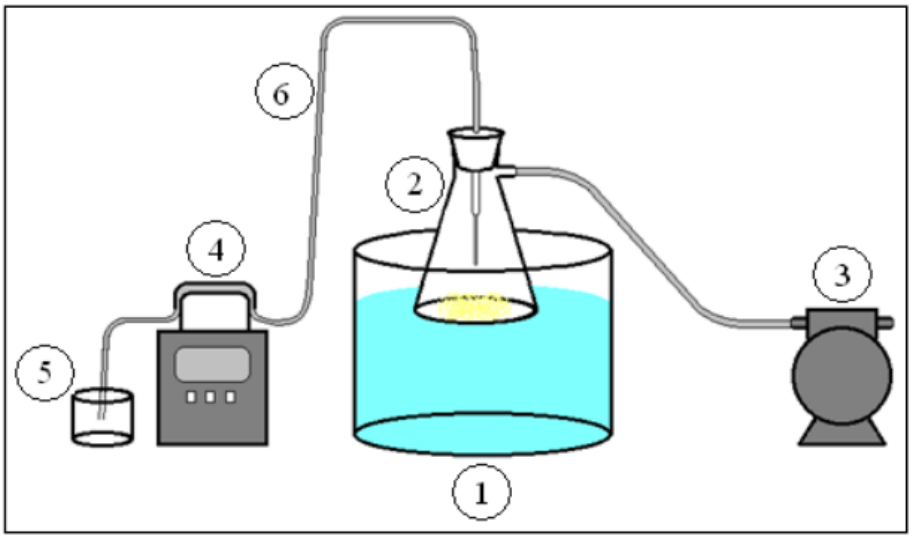

Figure 3.1. Schematic diagram of the impregnation system
(1. Ultrasonic mixer, 2. Büchner flask, 3. Vacuum pump, 4. Peristaltic pump, 5. Precursor solution, 6. Silicone tubing).

3.2.2. Catalyst Testing System

Autoclave Engineer's BTRS-Jr-PC with fixed bed tubular continuous flow reactor is combined within a fully automated reactor system and it is encased within one bench top unit as shown in Figures 3.3 and 3.4. This system consists of a 20 ml fixed-bed tubular continuous flow reactor that can withstand pressures and temperatures up to 100 bar and 650 ^{o}C, respectively. The reaction system, whose flow sheet is presented in Figure 3.5, has numerous sections that are described in the following sections.

3.2.2.1. Feed preparation section. Reactant feeds (Hydrogen, Carbon monoxide and Nitrogen) enter the system with carrier gas (Argon) and their delivery rates are controlled with dedicated mass flow controllers (Brooks Instrument Model number 5850TRG). Reactants then pass through the mixer and vaporizer unit where they are homogeneously mixed and heated to the desired temperature before the reaction.

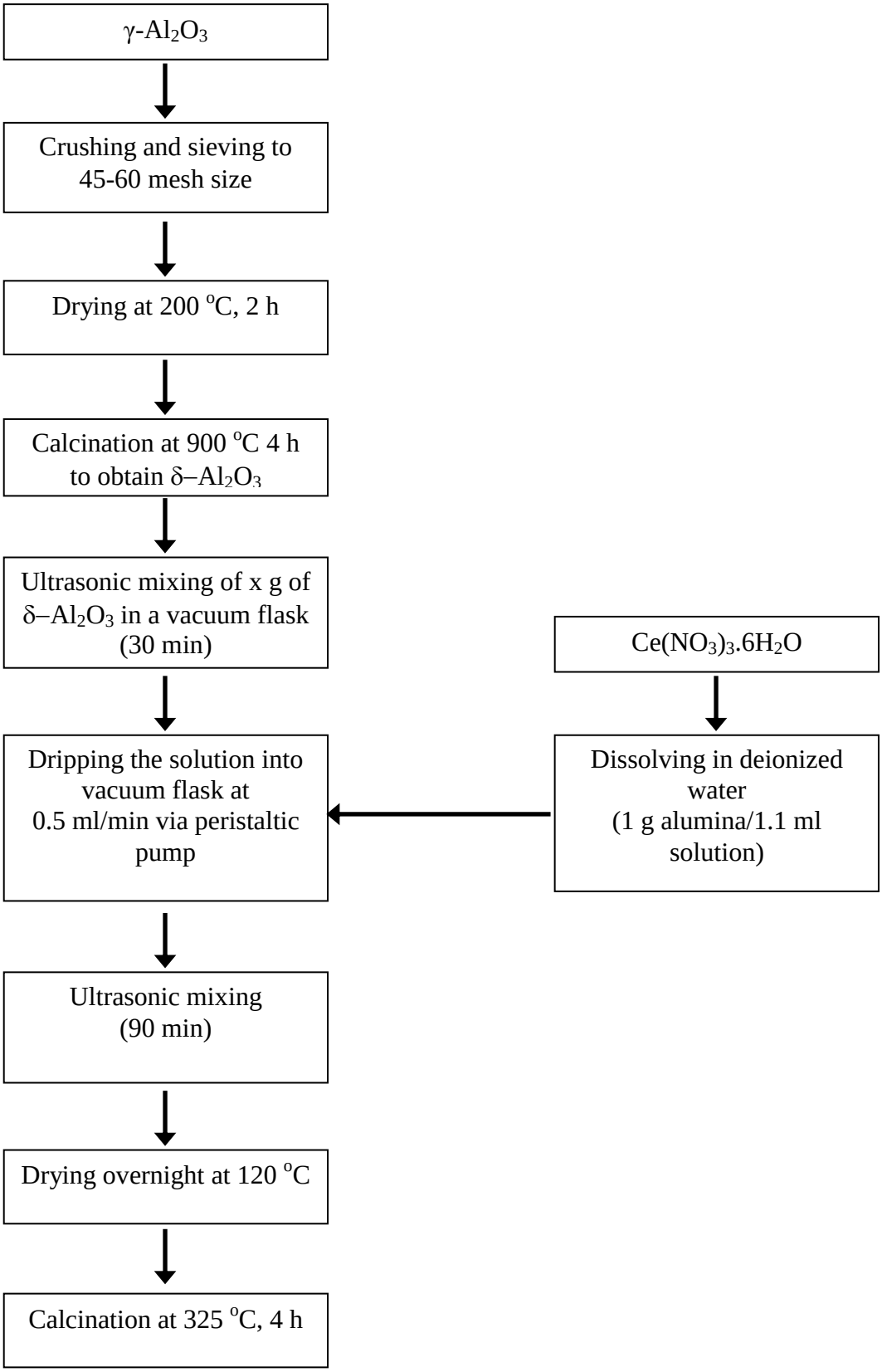

Figure 3.2. Preparation steps of CeO_2/δ-Al_2O_3 catalyst via incipient to wetness impregnation.

Figure 3.3. The Autoclave Engineer's BTRS-Jr-PC high-pressure fixed bed reactor system.

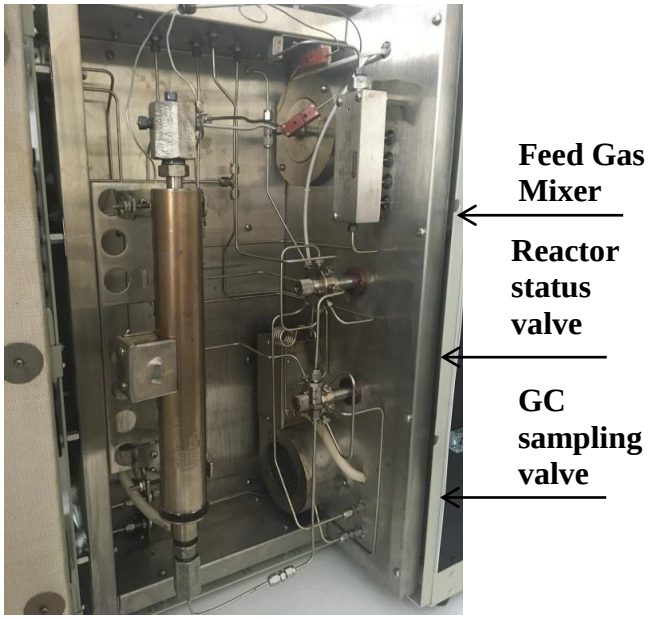

Figure 3.4. The Autoclave Engineer's BTRS-Jr-PC reactor oven cabinet.

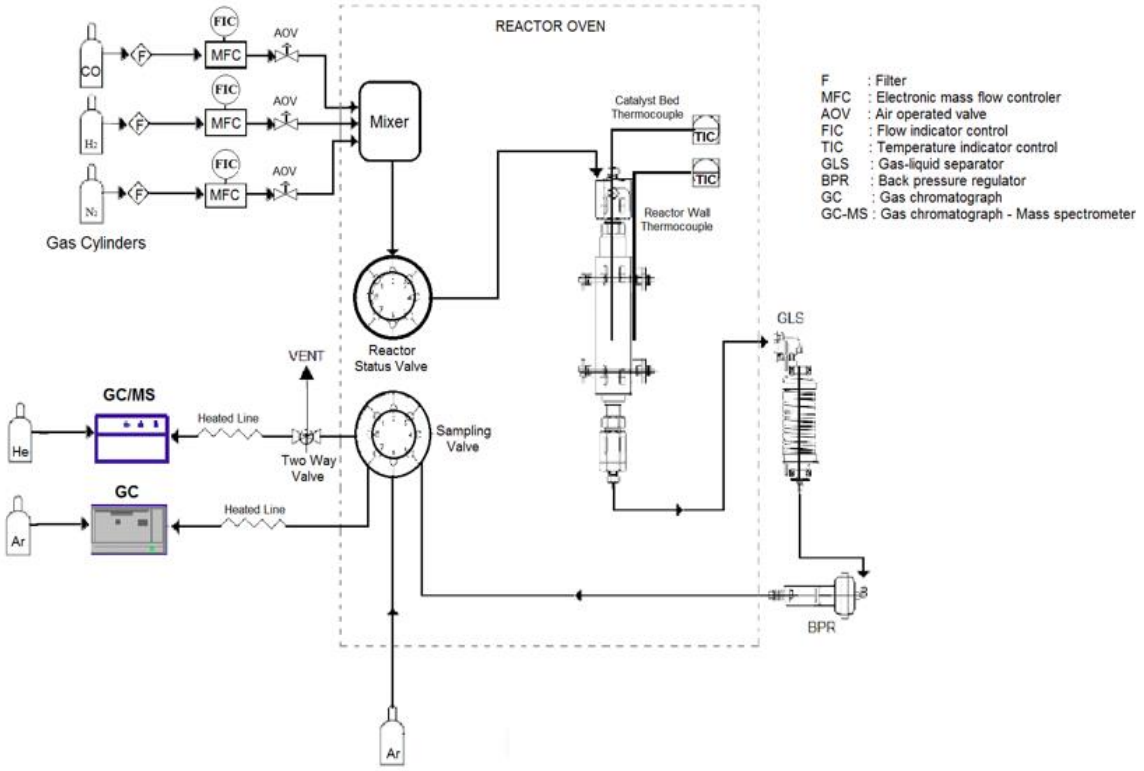

Figure 3.5. Flow sheet of the automated fixed bed reactor of BTRS-Jr-PC.

3.2.2.2. Reactor section. BTRS Jr-PC has one tubular reactor and furnace assembly all closed up in the reactor oven cabinet which is well-insulated and allows execution of the reactions at the desired temperature. Oven cabinet encloses the tubular reactor, tubings and switching valves (i.e. reactor status valve and gas chromatography sampling valve). In order to prevent condensation of the product stream leaving the reactor, the oven temperature is controlled at 150 °C. The tubular reactor is made of 316 stainless steel with dimensions of 7.65 mm (ID) x 14.05 mm (OD) x 4 cm (Length), resulting in a volume of 20 cm^3, and involves a ceramic heating jacket. Single zone electric resistance heater of the reactor is located at the outside of the ceramic heating jacket. Electric resistance heater has two K-type thermocouples, both of which are connected to the Programmable Logic Controller (PLC) for controlling the reactor temperature. The desired oven and reactor temperatures are set via a software (HMI), and controlled via PID mechanism. A screenshot of the HMI software is presented in Figure 3.6.

Reactor section also involves a 2-position 8-port valve, which is also called as reactor status valve, located in the reactor oven cabinet, which controls the path of the feed and product gases (Figure 3.4). Online and offline states of the reactor status valve divert the route of the gases to the desired position. In the online mode, feed gases go through the reactor and then enters gas liquid separator and effluent is discharged from the reactor purge vent. In the offline mode, which is preferred for feed analysis, reactant gases bypass the reactor and directly leave the system from the reactor vent. However, for this particular system it was found that there is an incorrectly set connection; when the system is 'on-line' it is displayed as 'off-line' in the HMI screen.

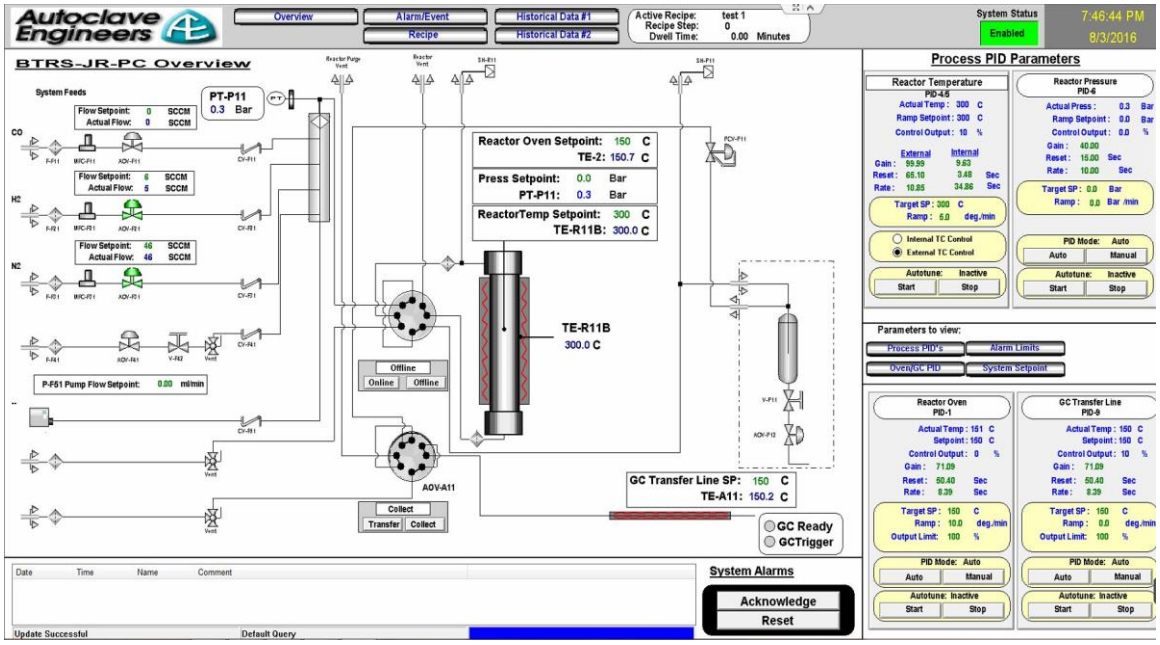

Figure 3.6. Screenshot of the HMI software used to control Autoclave Engineers' BTRS Jr-PC

3.2.2.3. Gas-Liquid Separator. Effluent gas of the reactor is passed through a gas-liquid separator (GLS) after leaving the reactor, which is a simply a heat exchanger. This unit is used to knock-down the condensable species in the reactor effluent. Control of the GLS is managed by the HMI screen with an air operated valve and metering valve located at the bottom of the GLS cabinet. Cooling of the gases that is directed to the shell-side of GLS with the cold water in the copper coils (i.e. tube side) of the heat exchanger is

supplied by an external circulating water bath (Nüve BS-302) with cooling function. However this section is decided not be used throughout the study since sometimes the amount of product gasses were too low to accumulate therefore on-line heated sampler line has been installed which is explained in detailed in Section 3.2.2.6.

3.2.2.4. Back pressure Regulator. Back pressure regulator is located on the top left hand side of the unit (Figure 3.3) and is the next unit that product mixtures pass through after the GLS. Control of the pressure at the set point and monitoring of the regulator is managed by PLC and isolated pressure gauge/transducer, respectively. Set point of the reactor pressure is entered by the HMI software.

3.2.2.5. Gas Chromatography (GC) Sampling Valve. After the back pressure regulator, product stream enter the GC sampling valve (Figure 3.7). GC sampling valve can be switched in to 'collect' and 'transfer' modes. In the collect mode product gas is directed to the vent through the sample loop which has an internal volume of 1 ml. In the transfer mode, on the other hand, the GC sampling valve pushes product gas in the sample loop to the online connected GC as can be seen in Figure 3.7.

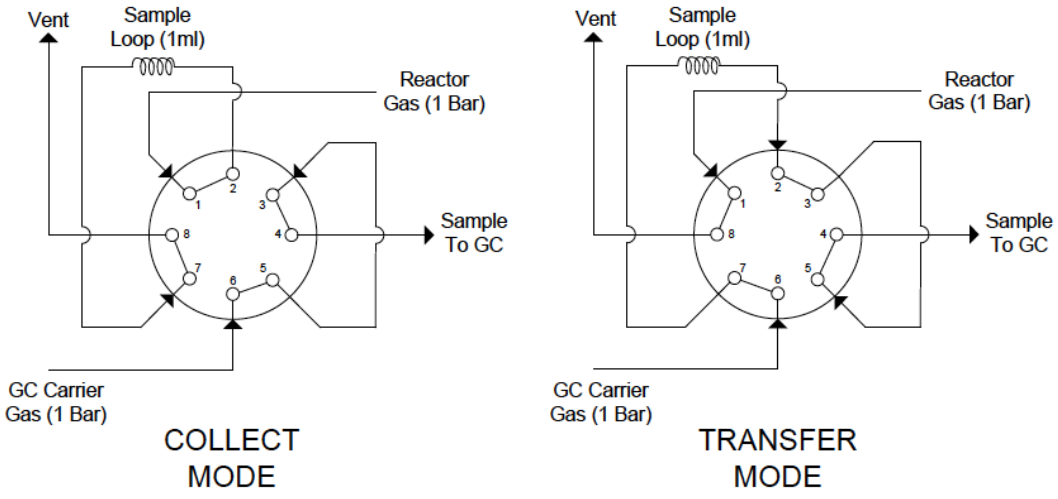

Figure 3.7. GC sampling valve configurations.

3.2.2.6. Transfer Lines. The system involves two online heated transfer lines for transferring gas samples to gas chromatography (GC) and gas chromatography-mass spectrometry (GC-MS) units (See Section 3.2.4). The GC sampling valve pushes the sample product gas to the GC via the heated transfer line, which is insulated stainless steel microbore tube, and its temperature can be controlled up to 180 °C from the HMI software. Transfer line is an integral part of the reaction system and, as mentioned above, it is connected to the GC unit. However, there is not a built-in online connection between the reaction system and the GC-MS, the second analysis unit involved in this study. Therefore, in order to transfer the reactor effluent to GC-MS, a heated, temperature controlled, stainless steel line is established between one of the outputs of a three-way valve attached to the reactor vent and the sampling valve of the GC-MS unit. This 5 m long, 1/8 in. ID line is wrapped with a heating tape and insulating layer. The heating tape is connected to an external heater which is powered by a digital on-off controller taking feedback from the mid-point of the line via a K-type sheathed thermocouple. The line can be heated up to ca. 100 °C to avoid condensation of the species in the product stream.

3.2.2.7. System Monitoring and Control. BTRS Jr-PC System functions are controlled by a Programmable Logic Controller (PLC) and HMI software (Figure 3.6) consecutively working on a standard desktop computer. These tools enable controlling the mass flow controllers, temperature (of the oven, reactor and the oven), pressure, and status of the reactor status and GC sampling valves. If the system gives an alarm warning, system alarms on the bottom of HMI screen turns into red and can be taken under control. Furthermore if the study is going to be held on over days then a proper recipe can be generated and loaded to the system to continue work according to the schedule.

3.2.3. System Commissioning and Experimental Procedure

3.2.3.1. Troubleshooting and Commissioning. BTRS Jr-PC and product analysis systems were set up in 2014 and re-commissioned for this study. At the very beginning of this study, the system was kept under N_2 flow for checking the functionality of both mechanical and electrical equipments, for the leak checks and for flushing the lines to clean up the possible dirt that could have accumulated by time.

After completion of the initial checks, the system was pressurized under N_2 flow. However the system pressure was unable to reach its set point, and was found to decrease with the N_2 flow rate. The problem was explained to control engineers at the Autoclave Engineers Operation, and it was advised to check any possible leaks. In order to avoid the leakage at the beginning of the experiments, the connecting nuts were over-tightened, which damaged the original shape of the nuts and made them almost impossible to tighten. Thus the nuts were decided to be replaced, but there were no spares available. Therefore the damaged nuts were removed and the line is re-assembled by Swagelok connections available in the lab. Therefore leakage problem was solved.

There was also a problem with the BTRS oven, which could not be heated by the standard operating procedure. The problem was transferred to the Autoclave Engineers again and it took ca. three weeks to understand the root cause of the problem, which was linked to the power switch of the oven. Since technical service from the Autoclave Engineers could only help with online connection from abroad, the solution was explained to us on the P&ID of the electrical circuit of the system. By using this information, the problem was eventually fixed by the department technician.

After the system was ensured to be work properly, the experiments were started. However, the GC data, which were periodically taken at each 45 min, were inconsistent with each other. In other words, the areas at one run turned out to be almost ten times higher than those obtained in the previous run. The problem was tried to be solved by doing many experiments to understand potential root causes of the problem such as the settings of GC unit or the method of reactor loading or the operating conditions. At the same time it was consulted to the Autoclave Engineers, and it was understood that the problem occurred due to unsteady pressure. The pressure could not reach to the set point of the pressure and stay approximately 2-3 bar below it. Thus, instead of N_2, reaction gases were used to stabilize the pressure, and, as a result, the amount of gas sample accumulated in the sampling valve turned out to be inconsistent in every analysis. The problem was eventually solved remotely by Autoclave Engineers, who made changes in the codes controls the system.

For carrying out analysis in the GC-MS unit, it was initially aimed to collect the product in the liquid form via draining from GLS at the end of the experiment. However, first there was a problem with the circulation of the water bath that was needed for the operation of GLS. This was fixed by a simple setting change in the circulation unit. Later on, the amount of liquid product was found to be very low in the GLS, most likely due to low conversions and amounts of material converted. Thus, it was decided to use the on-line connection to GC-MS (see Section 3.2.2.6). Therefore, the experiments were re-run and product distributions were obtained in a more consistent way.

It is worth noting that it took almost 3 months to understand the root causes of the problems listed above and implement their solution. The dependence on external suppliers and their sluggish responses delayed successful commissioning of the experimental set-up.

3.2.3.2. Experimental Procedure. The preparation of the reactor tube to loading was performed by first taking off thermocouples (one inside the jacket and the other inside the reactor) from the reactor inlet and heating jacket. Then the shaft (which is a cable connected to heating jacket which energize the reactor tube) is disconnected from the system and the nuts (which exist at both inlet and the outlet of the reactor and helps to have no leakage in the reactor) were disassembled from the reactor tube. Reactor tube is cleaned by the solvents according to sequence of distilled water, HCl (Hydrochloric acid), distilled water, ethanol and acetone. When the reactor tube was ensured to be clean, a certain amount of glass wool was pushed down in to the middle of the reactor with a thin tube since one of the thermocouples was located in the middle of the catalyst bed. After the insertion of the glass wool, 0.4 g of bi-functional catalyst were weighed and poured into the reactor with the help of an appropriate funnel. The catalysts were placed sequentially, that is packing of 0.2 g of methanol dehydration catalyst was followed by placing the methanol synthesis catalyst (HiFUEL R120). A second layer of glass wool was then inserted and packed on top of the catalyst bed to prevent and kind of fluidization. The important thing is not to press the glass wool with thin tube because then gas flow might not be homogeneous and then there might be pressure drop. Finally

when the reactor was loaded it was then re-assembled and re-connected to the system. Loading method is demonstrated in Figure 3.8.

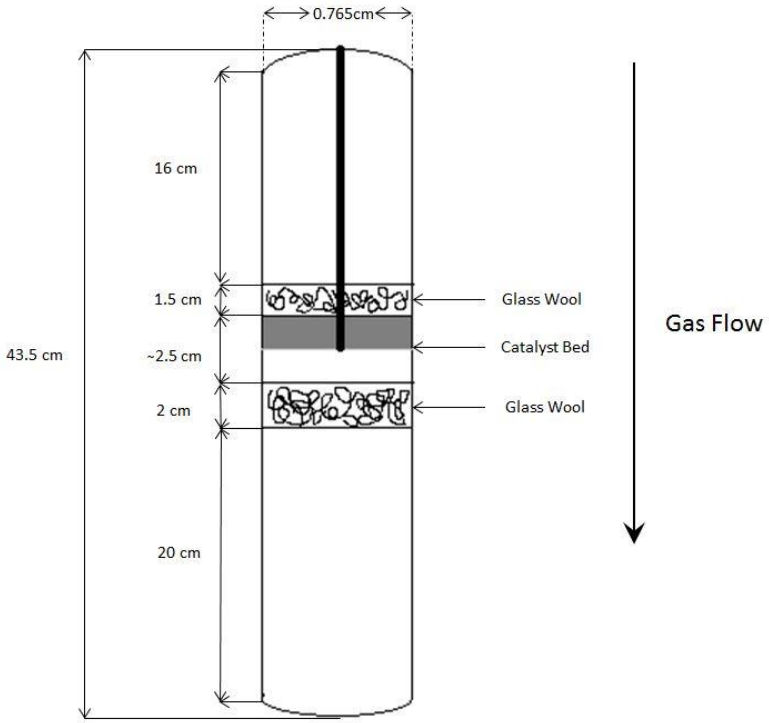

Figure 3.8. Loading method for the tubular reactor.

Initiation of a typical experiment initially involves increasing the temperature from the room temperature to 300 ^{o}C with a heating rate 5 ^{o}C/min under N_2 flow at 45 ml/min. When the set temperature is achieved, *in situ* reduction process is started with addition of 5ml/min $H_2$to $N_2$to obtain a total flow rate of 50 ml/min with a composition of 10% (by volume) H_2 and 90% N_2 at atmospheric pressure. Reduction process continues for 2h and after that, reactor temperature is allowed to stay constant or cooled down to reaction temperature under 45 ml/min N_2 flow for about 1h. Once the desired reaction temperature is obtained, total reactant flow rate is adjusted as 100 ml/min and its volumetric composition is set as 32/64/4 ($CO/H_2/N_2$) or 48/48/4 ($CO/H_2/N_2$) where the N_2 was used as internal standard in the feed. Based on these conditions, gas hourly space velocity and space-time are calculated as 15000 ml/gcat.h and 0.24 g.s/ml, respectively. Details of the experiments carried out in this study are presented in Table 3.4.

Table 3.4. Summary of the performed experiments and catalysts used.

Exp. No	**Catalyst type**	**Reaction Pressure (bar)**	**Reaction Temperature (^oC)**	**Feed composition in N_2 as balance**	
				CO (vol%)	H_2 (vol%)
1	HiFUEL R120-5% CeO_2/δ-Al_2O_3	34	250	32	64
2		34	275	32	64
3		34	300	32	64
4		25	300	32	64
5		34	300	48	48
6	HiFUEL R120-10% CeO2/δ-Al_2O_3	34	250	32	64
7		34	275	32	64
8		34	300	32	64
9		25	300	32	64
10		34	300	48	48
11	HiFUEL R120-20% CeO2/δ-Al_2O_3	34	275	32	64
12		34	300	32	64

3.2.4. Product Analysis Systems

Product analysis is carried out by a GC and a GC-MS unit. The GC (Shimazdu 2014) is used for quantitative analysis of CO, H_2, N_2, CO_2 and CH_4 via a thermal conductivity detector (TCD). Sampling to this unit is done by the GC sampling valve (Section 3.2.2.5) that is built-in in the reaction system. As explained above, transfer of the sample is done via a transfer line, which is also an integral part of the reaction

system. Transport of the 1 ml sample is achieved by Ar with a flow rate of 15 ml/min. Prior to its use, the GC unit is conditioned and calibrated by injecting certain binary mixtures of N_2, H_2 and CO whose relative amounts are metered precisely by the mass flow controllers of the reaction system (Section 3.2.2.1).

Calibration of the GC for CO_2 and CH_4 is carried out by injecting the pertinent component at certain amounts via a gas needle. Other properties of the GC unit and the operating conditions involved in it are presented in Table 3.5.

Table 3.5. Properties of and analysis conditions used in Shimadzu GC-2014 unit.

GC Property	**Attribute/Value**
Detector type	TCD
Column temperature	40 °C for 14 min, 40 -150 °C at 55 °C /min, 150 °C for 16 min
Injector temperature	100 °C
Detector temperature	175 °C
Carrier gas	Argon
Detector current	50 μA
Carrier gas flow rate	25 ml/min
Column packing material	Carboxen-1000, 80-60 mesh
Column tubing material	Stainless steel
Column length & ID	6 m & 3 mm

Analysis of dimethyl ether, CO, CO_2, CH_4 and other components that were not captured in the GC unit are analyzed in a Shimadzu GCMS-QP2010 unit. Outlet of the

reactor vent is passed through a heated line, which is connected to a manually activated heated-gas sampler (Shimadzu HGS-2) that involves a temperature controlled six-way valve with a sample loop volume of 1 ml. Injection of the gas sample, which is also heated for preventing condensation in the sample loop, to the GC-MS unit is carried out by HGS-2 unit. Operating conditions and properties of the GC-MS unit is given in Figure 3.6.

Table 3.6. Properties of and analysis conditions used in GCMS-QP2010.

GC-MS Property	**Attribute/Value**
Detector type	Mass Spectrometer Detector
Column type	Rt-Q-Bond Capillar
Carrier gas	Helium
Column length, ID and thickness	30 m, 0.53 mm and 20 μm
GC part	
Column temperature	35 ^{0}C for 5 min 35 -150 ^{0}C at 50 ^{0}C/min 150 ^{0}C for 10 min
Injector temperature	220 ^{0}C
Injection mode	Split
Column flow	3 ml/min
Split Ratio	50
Total analysis time	17.30 min
MS part	
Ion source temperature	220 ^{0}C
Scan speed	769 m/z
Solvent cut time	0.6 min

Calculations of the conversion, selectivity and yield of the gases were performed with the help of six successive data taken from the product analysis systems after the reaction reached steady state conditions, which is taken as 1h after the initiation of the reaction. CO conversion was calculated from the data taken from GC and DME, methanol, CH_4, CO_2 and other paraffins (C_2H_4, C_2H_6, $C3H_8$, C_4H_{10} and C_5H_{12}) selectivity were calculated from average of the data taken from GC-MS. However, consistency between GC and GC-MS was ensured by calculating CH_4 and CO_2 selectivity from the data taken from both analysis systems, which gave comparable outcomes.

CO conversion was defined based on the molar flow rates of CO both in the feed ($n_{CO,in}$) and in the product streams ($n_{CO,out}$) as follows;

$$X_{CO}\ (\%)\ =\ \left[\frac{n_{CO,in}-n_{CO,out}}{n_{CO,in}}\right]\times 100 \tag{3.1}$$

Selectivity of the products were expressed by the ratio of molar flow rates of each gas to the total moles of CO converted to the products, as given as;

$$S_{CO_2}(\%) = \left[\frac{n_{CO_2}}{n_{CO,in}-n_{CO,out}}\right]\times 100 \tag{3.2}$$

$$S_{CH_4}(\%) = \left[\frac{n_{CH_4}}{n_{CO,in}-n_{CO,out}}\right]\times 100 \tag{3.3}$$

The presence of DME, methanol and other paraffins was detected by GC-MS, but their yield and selectivity calculations necessitate calibrations for individual components. However, GC-MS calibration for these molecules was not so easy since GC-MS detector became saturated during analyzing the high purity substances. Due to the unavailability of standard mixtures that could be used for calibration, molar flow rates methanol and other paraffins of were calculated with following equation [62];

$$N_i = N_{ref} \frac{M_{ref}}{M_i} \frac{A_{ref}}{A_i} \frac{Q_{ref}}{Q_i} \quad (3.4)$$

where subscript "i" and "ref" correspond to the quantified species and reference compound, respectively. N is the number of moles of species, M is molecular weight and A is the area under the peak obtained from GCMS-QP2010. For methanol and other paraffins, methane is taken as reference compound. Q is total ionization cross section. The response factor could be defined as arbitrary peak area per mole of compound. Since the electron impact voltage of GC-MS is 70 eV, experimental values of total ionization cross sections for ethanol and methane corresponding this voltage were found in literature given in Table 3.7 [63,64].

Table 3.7. Total ionization cross section of the some compounds.

Compound	**Q (Total ionization cross section)**
CH_4	4.67
C_2H_4	6.93
C_2H_6	8.51
C_3H_8	10.5
C_4H_{10}	15.3
C_5H_{12}	18.6
CH_3OH	4.44

At first DME molar flow rate was also calculated from Equation 3.4. However since DME was a main product this approach was not found to be appropriate to use the method given in Equation 3.4 was proposed to quantify only small amounts of by-products whose peak areas are comparable with that of the reference component [62]. Therefore DME flow rate was determined from the carbon balance calculation. Using this method is expected to deliver correct outcomes since almost all of the carbon containing products could be analyzed via GC-MS, and no coke formation was observed

over the catalyst within the range of experimental conditions studied. Number of moles of paraffins other than CH_4 was calculated by Equation 3.4. Therefore, molar flow rate of the DME is obtained according to Equation 3.5 and 3.6 where N denotes the number of Carbon in the compound and n as molar flow rate of that compound.

$$N_{DME}n_{DME} = \left[(N_{CO}n_{CO,in-}N_{CO}n_{CO,out})_-(\ N_{CH_4}n_{CH_4} + N_{CO_2}n_{CO_2} + N_{CH_4OH}n_{CH_4OH} + \sum N_{Paraffins}n_{Paraffins})\right] \quad (3.5)$$

$$\sum N_{Paraffins}n_{Paraffins} = N_{C_2H_4}n_{C_2H_4} + N_{C_2H_6}n_{C_2H_6} + N_{C_3H_8}n_{C_3H_8} + N_{C_4H_{10}}n_{C_4H_{10}} + N_{C_5H_{12}}n_{C_5H_{12}} \quad (3.6)$$

After the calculation of the molar flow rate of the DME overall selectivity of DME is calculated as follows:

$$S_{DME}\,(\%) = \left[\frac{2 \times n_{DME}}{n_{CO,in-}n_{CO,out}}\right] \times 100 \quad (3.7)$$

Yield of the products are also calculated from the Equation 3.8 as follows:

$$Y_i = \frac{n_i}{n_{CO,in}} \times 100 \quad (3.8)$$

4. RESULTS AND DISCUSSIONS

Parametric study over DME synthesis activity properties of the bi-functional catalysts, which are commercial copper based methanol reforming HiFUEL R120 and CeO_2 impregnated δ-Al_2O_3, were examined through the conditions presented in Table 3.4. Effect of temperature, pressure and feed composition on 5 and 10% CeO_2/δ-Al_2O_3, and effect of temperature on 20% CeO_2/δ-Al_2O_3 were studied and also effect of levels of CeO_2 loading was investigated. In all cases, the tests were performed constant catalyst amount of 0.4 g (sequential loading with 0.2 g of CeO_2/δ-Al_2O_3 and 0.2 g HiFUEL R120, respectively) and at constant gas hourly space velocity and space-time of 15000 ml/(gcat.h) and 0.24 g.s/ml, respectively. The results were calculated according to definitions given in the Section 3.2.4.

4.1. Effect of Temperature

HiFUEL R120-5% CeO_2/ δ-Al_2O_3 was investigated throughout the examination of effect of temperature on catalytic activity of the DME synthesis. As can be seen from the Figure 4.1, when the temperature is increased the CO conversion has been also increased. This result goes along with study carried out by Imamura *et al.* (1999). In their study they reported that CO conversion increased with temperature and, among other methanol dehydration catalyst they have used, CeO_2 showed the highest activity. Methanol formation, on the other hand, was decreased at high temperatures since methanol synthesis reaction is an exothermic reaction. Furthermore, methane amount increased at high levels of temperature [39]. Catalytic activity with time-on-stream, illustrated in Figure 4.2, showed that CO conversion was slightly decreased throughout the reaction process at all three different temperatures. However, after 2h from the start-up of the reaction, CO conversions started to exhibit a stable behavior. This trend, which was valid at 250 and 275 °C, seemed to be disturbed at 300 °C, at which a monotonic decline in activity was noticed. The results indicate that, as of 300 °C, catalysts start to become deactivated, whose root causes are under investigation. One possible root cause is the

thermal stability of Cu-ZnO based HiFUEL catalysts, which is known to sinter at temperatures close to ca. 330 °C.

In Figure 4.3, these results were also observed, as the selectivity of the methanol was decreased whereas the selectivity of methane was increased with temperature. Diminishing overall methanol selectivity might also have caused the rise in the selectivity of DME according to following reactions:

$$3CO + 3H_2 \leftrightarrow CH_3OCH_3 + CO_2 \quad (2.2)$$

$$2CO + 4H_2 \leftrightarrow CH_3OCH_3 + H_2O \quad (2.3)$$

The yield of the main products and by-products were also calculated and presented in Table 4.2 and Table 4.3, respectively. CO_2 yield slightly increased with temperature, as illustrated in Table 4.2. This result, however, is in contrast with CO_2 selectivity, which decreased significantly with temperature (Table 4.3) and can be explained with the fact that at 300^oC reverse water-gas shift reaction might be favored to the reactant side to consume CO_2 in the reaction medium. This drop in selectivity was counterbalanced by multiplying it with conversion to obtain yield, which was found to be slightly higher at 300 °C (Table 4.2). Formation of C_{2+}hydrocarbons (C_2H_4, C_2H_6, C_3H_8, C_4H_{10} and C_5H_{12}) were found to occur at lower quantities (Table 4.3). The reason that their yields were relatively low was because the catalysts have been used in DME synthesis was more selective for methanol synthesis than the Fischer-Tropsch synthesis. It is also observed that yields of CH_4 and C_{2+} hydrocarbons respond oppositely with temperature. Promotion of CH_4 formation at higher temperatures is an expected and a commonly observed trend in CO hydrogenation studies.

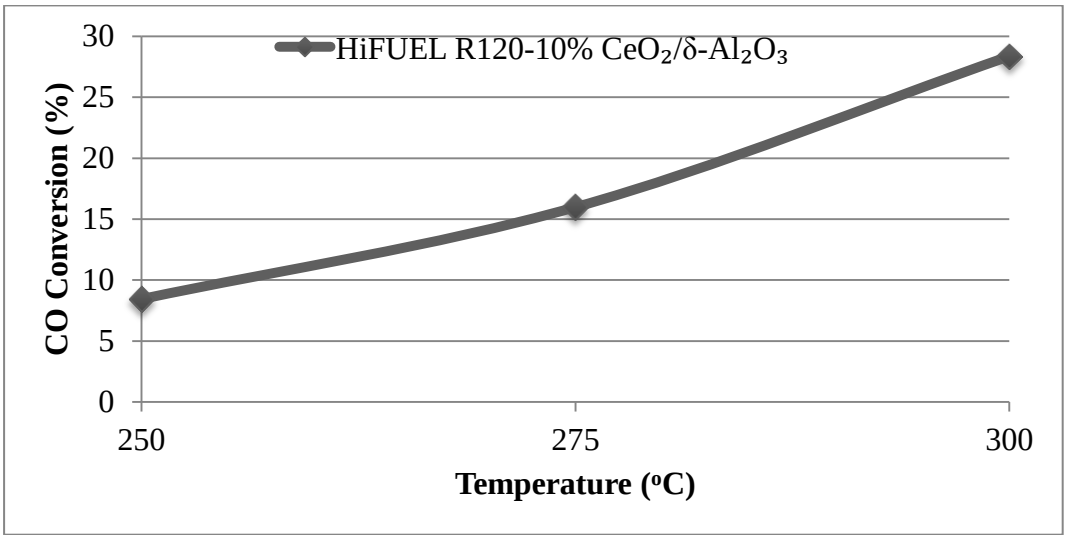

Figure 4.1. Effect of temperature on catalytic performance on HiFUEL R120-5% CeO_2/δ-Al_2O_3 ($CO/H_2/N_2$ =32/64/4, 34 bar).

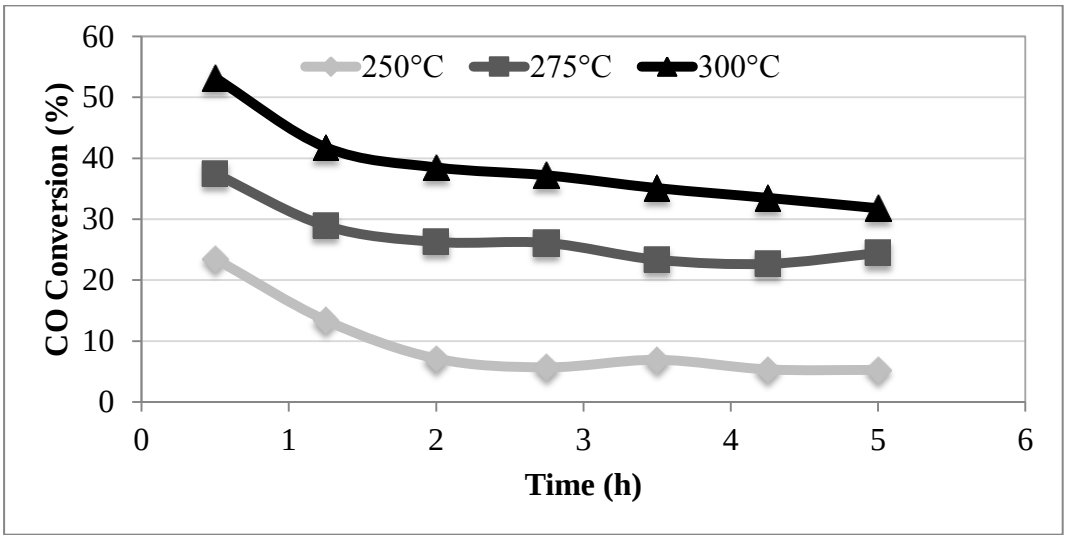

Figure 4.2. Temperature dependence of CO conversion with time-on-stream for HiFUEL R120-5% CeO_2/δ-Al_2O_3 ($CO/H_2/N_2$ =32/64/4, 34 bar).

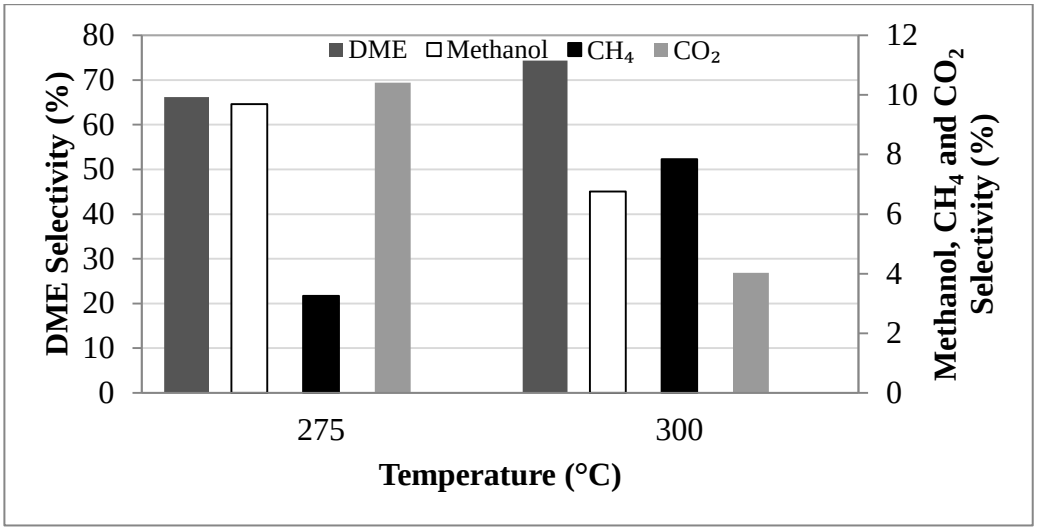

Figure 4.3. Temperature dependence of DME, methanol, CH_4 and CO_2 selectivity for HiFUEL R120-5% CeO_2/δ-Al_2O_3 ($CO/H_2/N_2$ =32/64/4, 34 bar).

Table 4.1. Selectivity of main products with HiFUEL R120-5% CeO_2/δ-Al_2O_3 at 275 °C and 300 °C ($CO/H_2/N_2$ =32/64/4, 34 bar).

Temperature (^oC)	DME selectivity (%)	Methanol selectivity (%)	CH_4 selectivity (%)	CO_2 selectivity (%)
275	66.2	10.7	4.0	14.7
300	74.4	6.8	7.8	4.0

Table 4.2. Yield of main products with HiFUEL R120-5% CeO_2/δ-Al_2O_3 at 275 °C and 300 °C ($CO/H_2/N_2$ =32/64/4, 34 bar).

Temperature (^oC)	DME yield (%)	Methanol yield (%)	CH_4 yield (%)	CO_2 yield (%)
275	8.9	2.6	0.9	2.8
300	14.4	2.6	1.6	3.0

Table 4.3. Yield of by-products with HiFUEL R120-5% CeO_2/δ-Al_2O_3 at 275 °C and 300 °C ($CO/H_2/N_2$ =32/64/4, 34 bar).

Temperature (°C)	C_2H_4 yield (%)	C_2H_6 yield (%)	C_3H_8 yield (%)	C_4H_{10} yield (%)	C_5H_{12} yield (%)
275	$8.2x10^{-2}$	$3.4x10^{-1}$	$4.0x10^{-1}$	$1.1x10^{-1}$	$4.7x10^{-1}$
300	$8.0x10^{-2}$	$5.4x10^{-1}$	$3.1x10^{-1}$	$5.5x10^{-2}$	$6.1x10^{-2}$

Effect of temperature on the response of HiFUEL R120-10% CeO_2/δ-Al_2O_3 catalyst combination is also studied. The outcomes, presented in Figures 4.4-4.6 and in Tables 4.4-4.6, show that the responses of the 10% CeO_2/δ-Al_2O_3 catalyst against change in temperature are qualitatively the same as those presented and discussed for the 5% CeO_2/δ-Al_2O_3.The only minor qualitative difference is observed in CO_2 yield, which was found to decrease slightly with temperature. As discusses earlier, CO_2 is a product of water-gas shift, which is an exothermic equilibrium reaction and shifts is the direction of CO_2 consumption with temperature [65]. This outcome, which is clearly observed in CO_2 selectivity reported in Table 4.4, is also reflected to its yield. In this case, increase in conversion turned out to be insufficient to elevate CO_2 yield.

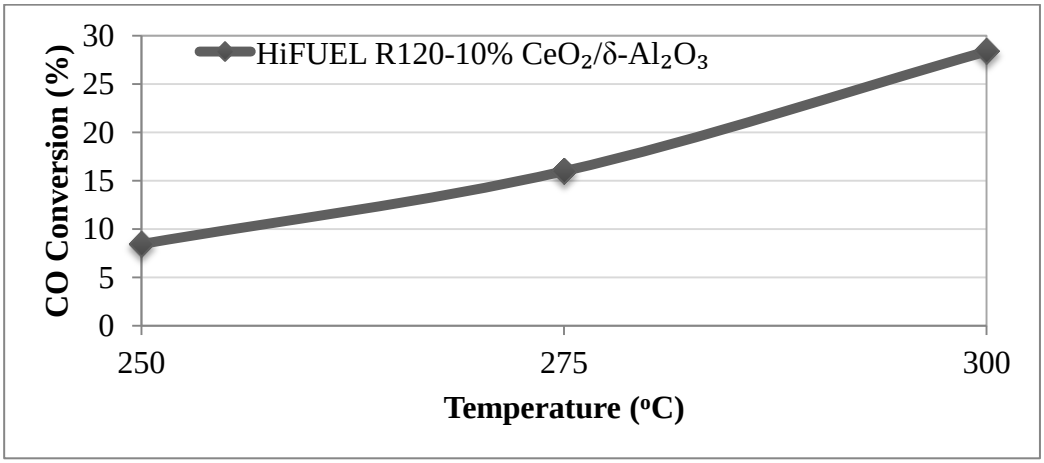

Figure 4.4. Effect of temperature on catalytic performance on HiFUEL R120-10% CeO_2/δ-Al_2O_3 ($CO/H_2/N_2$ =32/64/4, 34 bar).

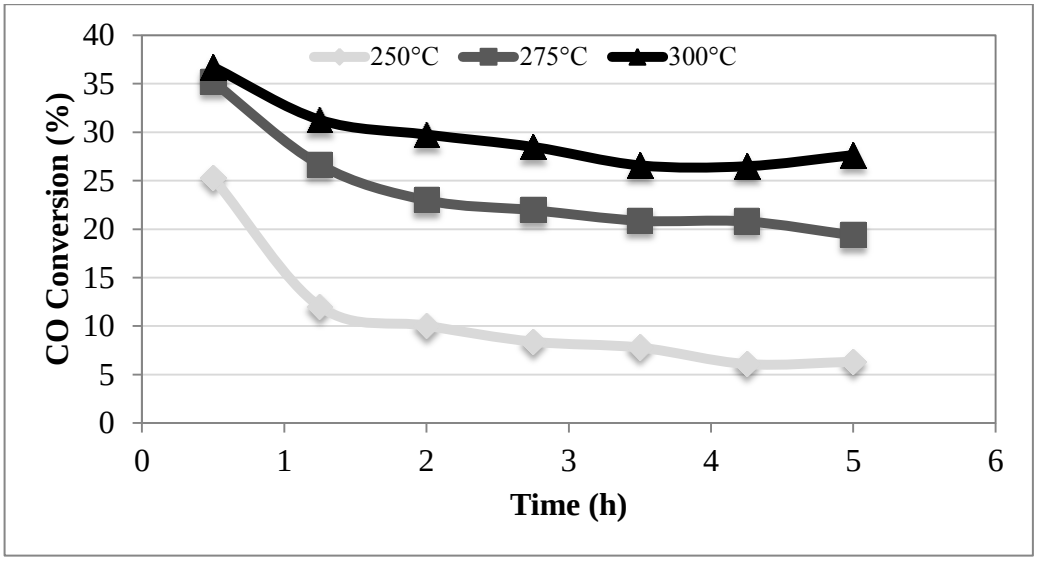

Figure 4.5. Temperature dependence of CO conversion with time-on-stream for HiFUEL R120-10% CeO_2/δ-Al_2O_3 ($CO/H_2/N_2$ =32/64/4, 34 bar).

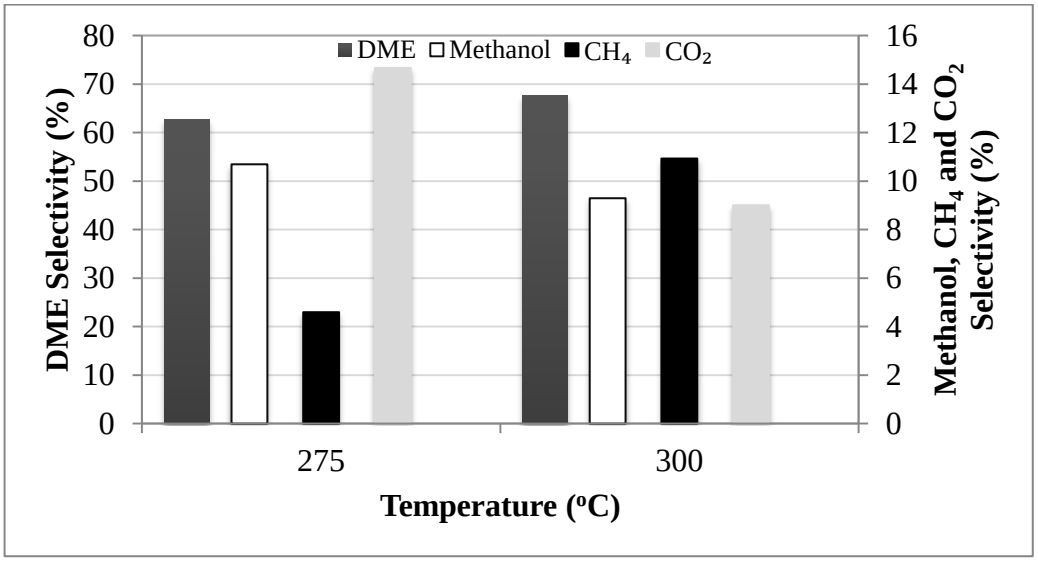

Figure 4.6. Temperature dependence of DME, methanol, CH_4 and CO_2 selectivity for HiFUEL R120-10% CeO_2/δ-Al_2O_3 ($CO/H_2/N_2$ =32/64/4, 34 bar)

Table 4.4. Selectivity of main products with HiFUEL R120-10% CeO_2/δ-Al_2O_3 at 275 and 300 °C ($CO/H_2/N_2$ =32/64/4, 34 bar).

Temperature (°C)	DME selectivity (%)	Methanol selectivity (%)	CH_4 selectivity (%)	CO_2 selectivity (%)
275	62.6	10.7	4.6	14.7
300	67.7	9.3	10.9	9.0

Table 4.5. Yield of main products with HiFUEL R120-10% CeO_2/δ-Al_2O_3 at 275 and 300 °C ($CO/H_2/N_2$ =32/64/4, 34 bar).

Temperature (°C)	DME yield (%)	Methanol yield (%)	CH_4 yield (%)	CO_2 yield (%)
275	8.1	2.8	1.2	2.7
300	10.0	2.8	3.1	2.6

Table 4.6. Yield of by-products with HiFUEL R120-10% CeO_2/δ-Al_2O_3 at 275 and 300 °C ($CO/H_2/N_2$ =32/64/4, 34 bar)

Temperature (°C)	C_2H_4 yield (%)	C_2H_6 yield (%)	C_3H_8 yield (%)	C_4H_{10} yield (%)	C_5H_{12} yield (%)
275	6.10×10^{-2}	3.31×10^{-1}	3.31×10^{-1}	1.02×10^{-1}	5.52×10^{-2}
300	1.01×10^{-2}	8.29×10^{-2}	1.37×10^{-1}	7.31×10^{-2}	1.01×10^{-2}

In addition to 5 and 10% ceria loaded catalysts, effect of temperature on the response of HiFUEL R120-20% CeO_2/δ-Al_2O_3 catalyst combination is also studied and reported in Figures 4.7 and 4.9, and in Tables 4.7-4.9. The opposite trend between DME and methanol selectivity was also noted clearly over the 20% CeO_2/δ-Al_2O_3 catalyst. This common trend shows that temperature elevation promotes simultaneous consumption of methanol and production of DME. This finding might result from the difference in the rates of methanol formation and dehydration, the latter being expected to become faster with temperature. In contrast with other catalysts, the change in conversions obtained over 20% ceria loaded one was found to be very limited. It is worth noting that due to the expectations of very low conversions, experiments at 250 °C were not carried out for 20% CeO_2/δ-Al_2O_3. This observation might be linked to a possible slight deactivation of the catalyst at 300 °C due to metal (i.e. ceria) sintering. Owing to the fact that the gap between the conversions obtained at 275 and 300 °C become less with increased ceria loading, the scenario of a possible, but limited metal sintering turns out to become realistic.

Another difference of the 20% ceria loaded catalyst was observed in CO_2 selectivity, which was found to increase with temperature. A possible explanation of this trend, which was just the opposite of those observed in other catalysts (Table 4.1 and Table 4.4), could be based on the amount of ceria, which catalytically counterbalanced the opposing effect of thermodynamics of water-gas shift reaction in the forward direction. It is worth noting that ceria is a highly effective promoter used in the catalysis of water-gas shift. Finally, as reported in previous cases, yields of C_{2+} hydrocarbons turned out to be very limited compared to those of DME, methanol and CH_4.

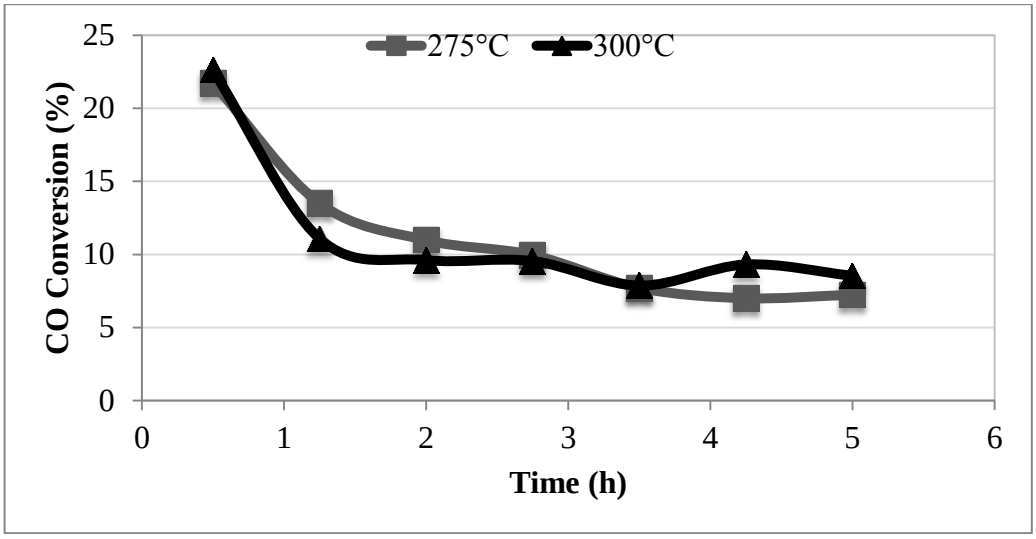

Figure 4.7. Effect of temperature on catalytic performance on HiFUEL R120-20% CeO_2/δ-Al_2O_3 ($CO/H_2/N_2$=32/64/4, 34 bar).

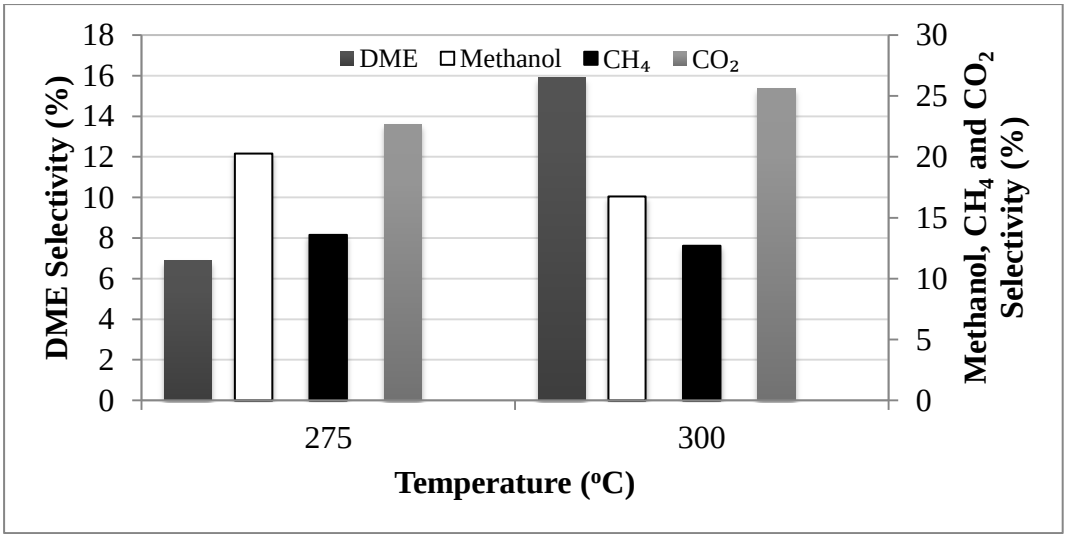

Figure 4.8. Temperature dependence of DME, methanol, CH_4 and CO_2 selectivity for HiFUEL R120-20% CeO_2/δ-Al_2O_3 ($CO/H_2/N_2$ =32/64/4, 34 bar).

Table 4.7. Selectivity of main products with HiFUEL R120-20% CeO_2/δ-Al_2O_3 at 275 and 300 ^oC ($CO/H_2/N_2$ =32/64/4, 34 bar).

Temperature (°C)	DME selectivity (%)	Methanol selectivity (%)	CH_4 selectivity (%)	CO_2 selectivity (%)
275	6.9	20.3	13.6	22.7
300	15.9	16.7	12.7	25.6

Table 4.8. Yield of main products with HiFUEL R120-20% CeO_2/δ-Al_2O_3 at 275 and 300 ^oC ($CO/H_2/N_2$ =32/64/4, 34 bar).

Temperature (°C)	DME yield (%)	Methanol yield (%)	CH_4 yield (%)	CO_2 yield (%)
275	0.4	2.3	1.5	2.5
300	0.9	1.9	1.4	2.9

Table 4.9. Yield of by-products with HiFUEL R120-20% CeO_2/δ-Al_2O_3 at 275 and 300 ^oC ($CO/H_2/N_2$ =32/64/4, 34 bar).

Temperature (°C)	C_2H_4 yield (%)	C_2H_6 yield (%)	C_3H_8 yield (%)	C_4H_{10} yield (%)	C_5H_{12} yield (%)
275	1.14	3.6×10^{-2}	4.1×10^{-1}	1.2×10^{-1}	7.1×10^{-3}
300	7.0×10^{-2}	5.5×10^{-1}	4.6×10^{-1}	1.4×10^{-1}	1.4×10^{-2}

4.2. Effect of Pressure

Reaction pressure is another parameter whose effect of conversion and product distribution is studied and reported in Figures 4.9-4.12 and in Tables 4.10-4.15. The experiments are carried out at 300 ^{o}C over HiFUEL R120-5% CeO_2/δ-Al_2O_3 and HiFUEL R120-10% CeO_2/δ-Al_2O_3 catalyst configurations. The results presented in Figure 4.9 show that, regardless of ceria loading, when the pressure was increased to 34 bar there is a sharp increase in CO conversion. This outcome can be explained by the thermodynamic considerations, since methanol synthesis (Reaction 2.4), which is the first step of thel overall reaction, is thermodynamically favored at high levels of pressure [66,67].

$$CO + 2H_2 \leftrightarrow CH_3OH \quad (2.4)$$

$$CH_3OH \leftrightarrow CH_3OCH_3 + CO_2 \quad (2.5)$$

$$CO + H_2O \leftrightarrow CO_2 + H_2 \quad (2.6)$$

Selectivity of the main products was illustrated in Figure 4.10 and in Table 4.10, which show that DME and methanol selectivity increase and decrease, respectively with pressure. It is worth noting that, among the key reactions (2.4)-(2.6) listed above, only methanol synthesis can be thermodynamically affected by pressure change. Even though this fact implies increased synthesis of methanol, its selectivity is found to respond oppositely with pressure. This fact can be related to the possible difference in the rates of methanol synthesis and dehydration, the latter being faster to transform higher quantities of methanol into DME via Reaction (2.5).

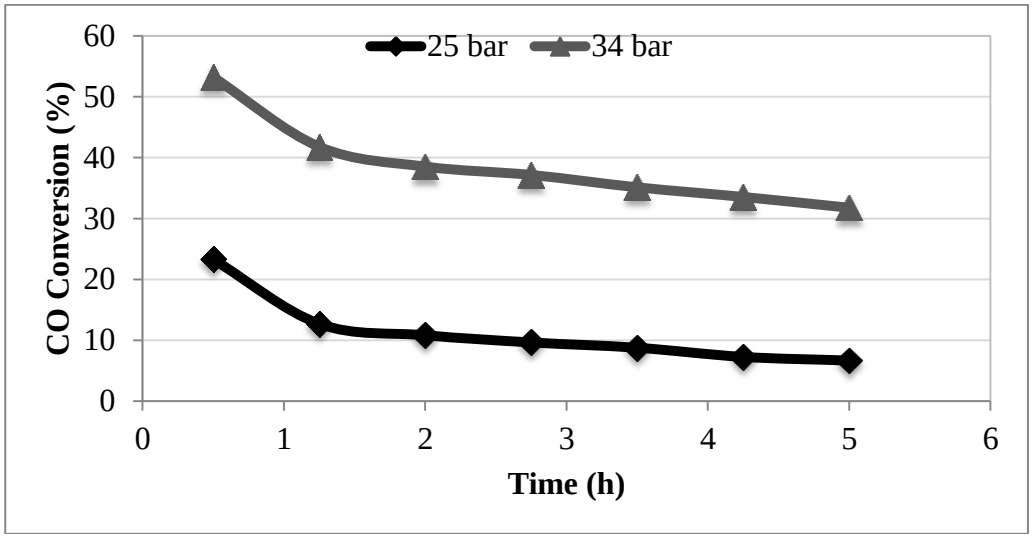

Figure 4.9. Pressure dependence of CO conversion with time-on-stream for HiFUEL R120-5% CeO_2/δ-Al_2O_3 ($CO/H_2/N_2$ =32/64/4, 34 bar).

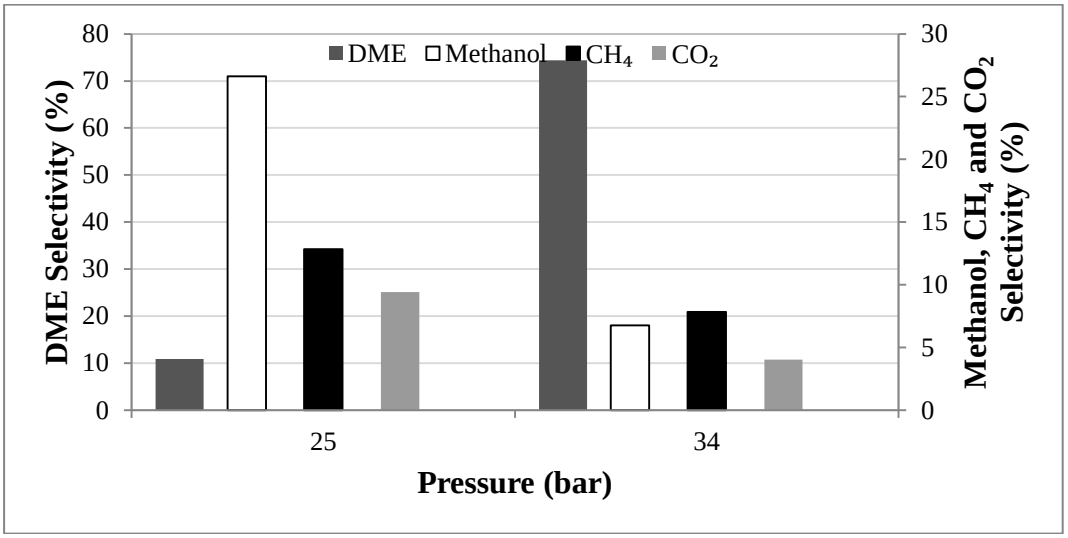

Figure 4.10. Pressure dependence of DME, methanol, CH_4 and CO_2selectivity for HiFUEL R120-5% CeO_2/δ-Al_2O_3 ($CO/H_2/N_2$ =32/64/4, 300 ^oC).

Table 4.10. Selectivity of main products with HiFUEL R120-5% CeO_2/δ-Al_2O_3 at 25 and 34 bar ($CO/H_2/N_2$ =32/64/4, 34 bar).

Pressure (bar)	DME selectivity (%)	Methanol selectivity (%)	CH_4 selectivity (%)	CO_2 selectivity (%)
25	10.9	26.6	12.8	9.4
34	74.4	6.8	7.8	4.0

Table 4.11. Yield of main products with HiFUEL R120-5% CeO_2/δ-Al_2O_3 at 25 and 34 bar ($CO/H_2/N_2$ =32/64/4, 34 bar).

Temperature (°C)	DME yield (%)	Methanol yield (%)	CH_4 yield (%)	CO_2 yield (%)
275	0.8	3.4	1.3	3.6
300	14.4	2.6	1.6	3.0

Table 4.12. Yield of by-products with HiFUEL R120-5% CeO_2/δ-Al_2O_3at 25 and 34 bar ($CO/H_2/N_2$ =32/64/4, 34 bar).

Pressure (bar)	C_2H_4 yield (%)	C_2H_6 yield (%)	C_3H_8 yield (%)	C_4H_{10} yield (%)	C_5H_{12} yield (%)
25	4.9×10^{-2}	4.2×10^{-1}	4.5×10^{-1}	1.3×10^{-1}	4.1×10^{-3}
34	1.01×10^{-2}	8.29×10^{-2}	1.37×10^{-1}	7.31×10^{-2}	1.01×10^{-2}

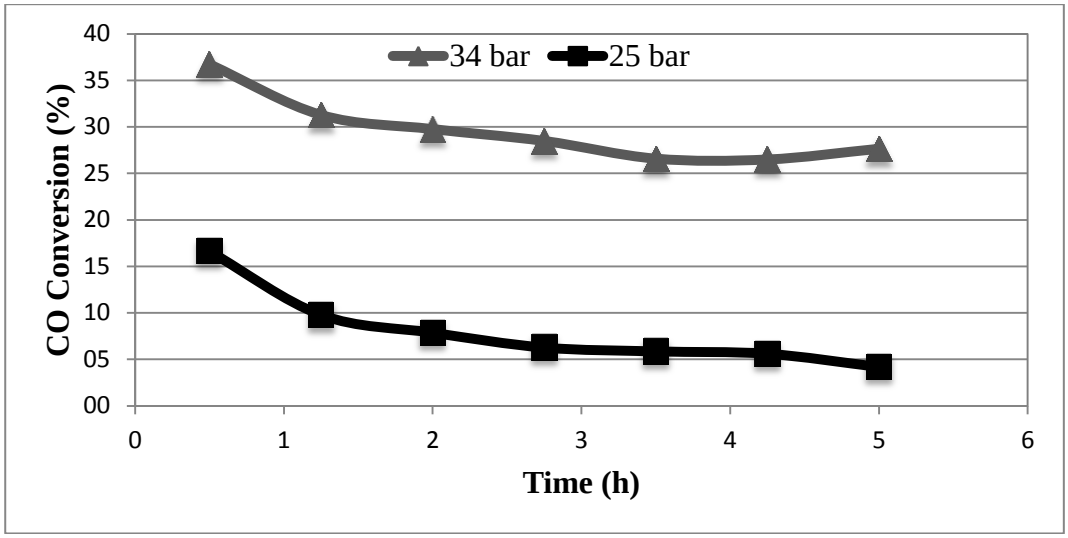

Figure 4.11. Pressure dependence of CO conversion with time-on-stream for HiFUEL R120-10 % CeO_2/ δ-Al_2O_3 ($CO/H_2/N_2$ =32/64/4, 34 bar).

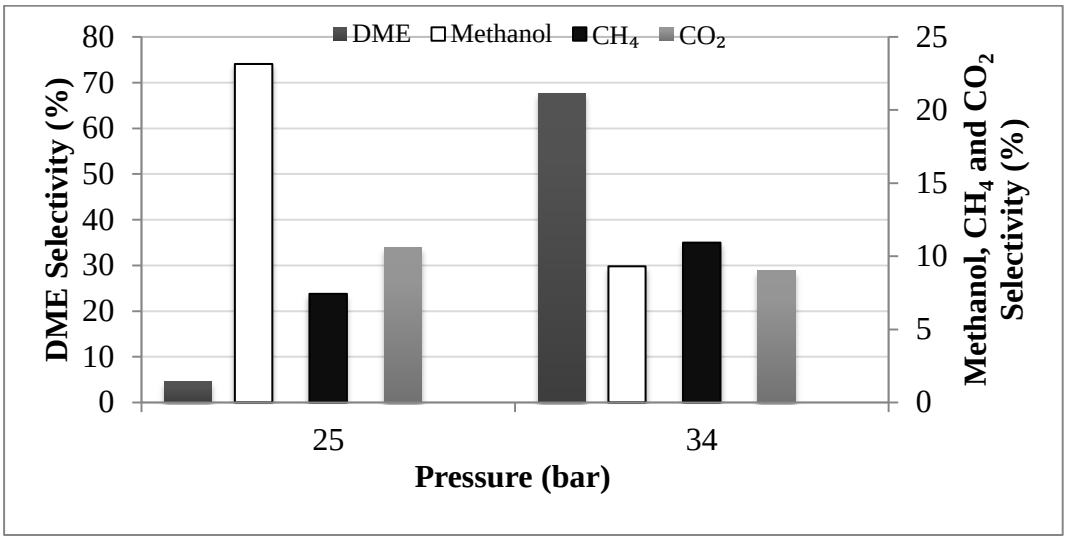

Figure 4.12. Pressure dependence of DME, CH_4 and CO_2 selectivity for HiFUEL R120-10% CeO_x/ δ-Al_2O_3 ($CO/H_2/N_2$ =32/64/4, 300 ^oC)

Table 4.13. Selectivity of main products with HiFUEL R120-10 % CeO_2/ δ-Al_2O_3 at 25 and 34 bar ($CO/H_2/N_2$ =32/64/4, 34 bar).

Pressure (bar)	DME selectivity (%)	Methanol selectivity (%)	CH_4 selectivity (%)	CO_2 selectivity (%)
25	4.5	23.1	7.4	10.6
34	67.7	9.3	10.9	9.0

Table 4.14. Yield of main products with HiFUEL R120-10 % CeO_2/ δ-Al_2O_3 at 25 and 34 bar ($CO/H_2/N_2$ =32/64/4, 34 bar).

Pressure (bar)	DME yield (%)	Methanol yield (%)	CH_4 yield (%)	CO_2 yield (%)
25	0.2	1.9	0.9	0.6
34	10.0	2.8	3.1	2.6

Table 4.15. Yield of by-products with HiFUEL R120-10 % CeO_2/ δ-Al_2O_3 at 25 and 34 bar ($CO/H_2/N_2$ =32/64/4, 34 bar).

Pressure (bar)	C_2H_4 yield (%)	C_2H_6 yield (%)	C_3H_8 yield (%)	C_4H_{10} yield (%)	C_5H_{12} yield (%)
25	6.5×10^{-2}	9.6×10^{-1}	7.2×10^{-1}	1.6×10^{-2}	1.7×10^{-2}
34	1.0×10^{-2}	8.3×10^{-2}	1.4×10^{-1}	7.3×10^{-2}	3.3×10^{-3}

4.3. Effect of Feed Composition

The effect of feed composition on CO conversion and product distribution was studied by changing the molar inlet H_2/CO ratio from 2, the default value, to 1. H_2/CO ratios of 1 and 2 were obtained by regulating the feed composition as H_2/CO/N_2 = 48/48/4 (by mole) and 64/32/4, respectively. These experiments were carried out at 34 bar and 300 ^oC over HiFUEL R120-5% CeO_2/δ-Al_2O_3 and HiFUEL R120-10% CeO_2/δ-Al_2O_3 catalyst configurations. The results obtained over both catalysts show that decreasing H_2/CO ratio from 2 to 1 caused notable reductions in conversion (Figures 4.13 and 4.15) and DME selectivity (Figures 4.14 and 4.16, and Tables 4.17 and 4.19). These findings can be linked to the impact of feed ratio on the thermodynamics of the reactions. Changing the feed ratio from 2 to 1 corresponds to a decrease in the total number of moles of CO and H_2 in methanol synthesis (Reaction 2.4) and shifts the reaction in the direction of methanol consumption. This effect would also shift methanol dehydration (Reaction 2.5) to the left, and favor consumption of DME and H_2O. Reduced quantities of steam would then shift the water-gas shift (Reaction 2.6) to the left. However, considering the fact that decreasing H_2/CO ratio is realized by increasing H_2 and decreasing CO amounts simultaneously, the overall change in the water-gas shift would be towards product side. Based on the discussion above, using H_2/CO = 1 would decrease CO conversion, DME selectivity and increase CO_2 selectivity, as reported for both catalysts in Figures 4.13-4.16 and in Tables 4.17 and 4.19.

In contrast with those of other major species, CH_4 selectivity was found to exhibit different responses to feed composition over 5 and 10% ceria loaded catalysts. Assuming that CH_4 formation occurs via CO hydrogenation (i.e. $CO + 3H_2 = CH_4 + H_2O$), decreasing H_2/CO ratio from 2 to 1 should shift the equilibrium to the left, i.e in the direction of CH_4 consumption. In such a case, CH_4 selectivity should decrease with H_2/CO ratio, as observed in the 10% ceria-loaded catalyst (Figure 4.16 and Table 4.19). Since this is not the case on 5% ceria-loaded catalyst, it is believed that some other reactions of methane formation occur within the reaction system. Finally, the yields reported for C_{2+} hydrocarbons in Tables 4.18 and 4.21 indicate that extent of by-product formation is small.

Table 4.16. Selectivity of main products with HiFUEL R120-5% CeO_2/δ-Al_2O_3 at different inlet H_2/CO ratios (300^oC, 34 bar).

Feed Composition (H_2/CO)	DME selectivity (%)	Methanol selectivity (%)	CH_4 selectivity (%)	CO_2 selectivity (%)
1	4.2	15.5	20.1	18.5
2	74.4	6.8	7.8	4.0

Table 4.17. Yield of main products with HiFUEL R120-5% CeO_2/δ-Al_2O_3 at different inlet H_2/CO ratios (300 ^oC, 34 bar).

Feed Composition (H_2/CO)	DME yield (%)	Methanol yield (%)	CH_4 yield (%)	CO_2 yield (%)
1	0.3	1.8	2.4	2.2
2	14.4	2.6	1.6	3.0

Table 4.18. Yield of by-products with HiFUEL R120-5% CeO_2/δ-Al_2O_3 at different inlet H_2/CO ratios (300^oC, 34 bar).

Feed Composition (H_2/CO)	C_2H_4 yield (%)	C_2H_6 yield (%)	C_3H_8 yield (%)	C_4H_{10} yield (%)	C_5H_{12} yield (%)
1	3.7×10^{-2}	1.2×10^{-1}	8.9×10^{-1}	3.1×10^{-1}	1.4×10^{-1}
2	8.0×10^{-2}	5.4×10^{-1}	3.1×10^{-1}	5.5×10^{-2}	6.1×10^{-2}

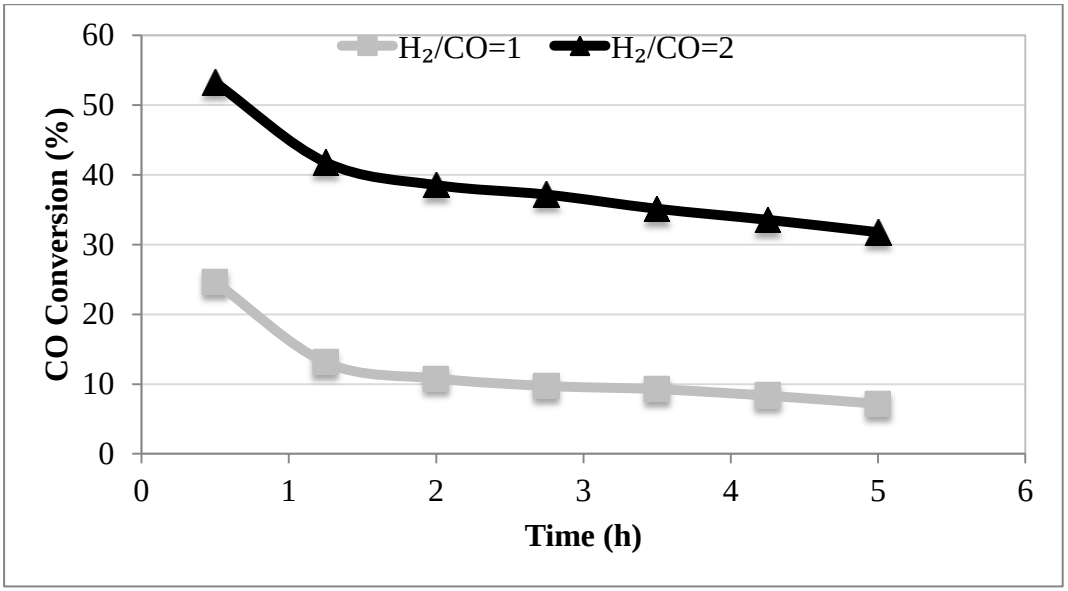

Figure 4.13. Feed composition (H_2/CO) dependence of CO conversion with time-on-stream for HiFUEL R120-5% CeO_2/δ-Al_2O_3 (CO/H_2/N_2 =32/64/4, 34 bar).

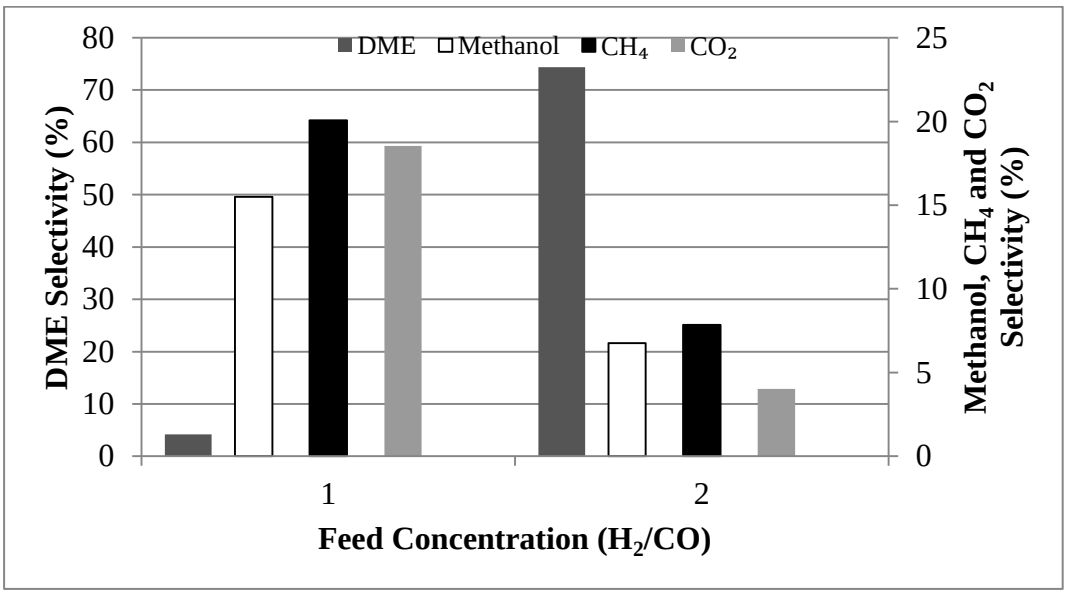

Figure 4.14. Feed composition (H_2/CO) dependence of DME, methanol, CH_4 and CO_2 conversion with time-on-stream for HiFUEL R120-5% CeO_2/□-Al_2O_3 (CO/H_2/N_2=32/64/4, 34 bar.

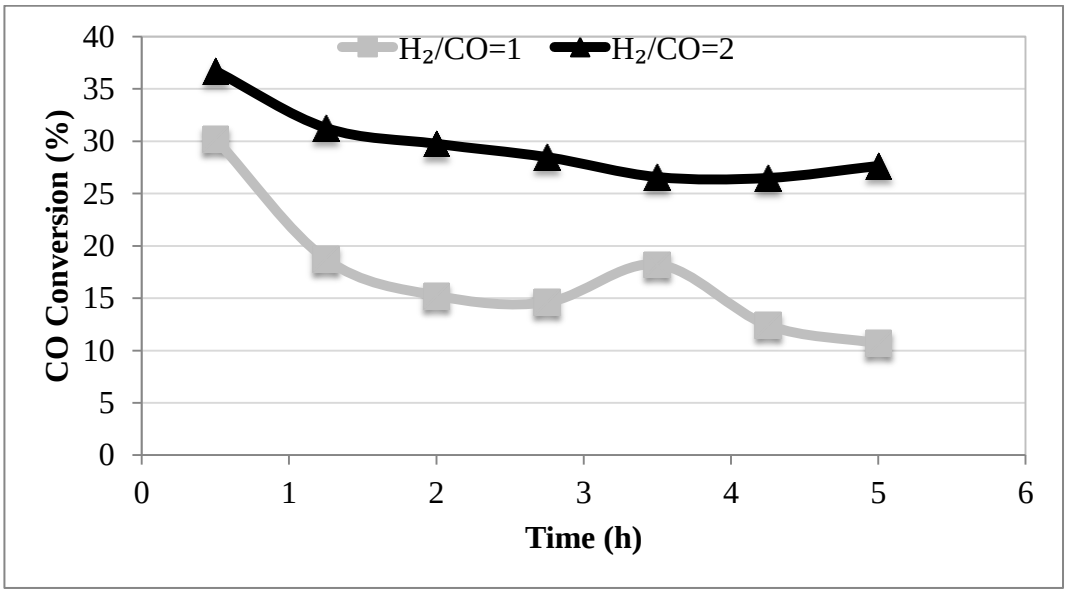

Figure 4.15. Feed composition (H_2/CO) dependence of CO conversion with time-on-stream for HiFUEL R120-10% CeO_2/δ-Al_2O_3 (CO/H_2/N_2 =32/64/4, 34 bar).

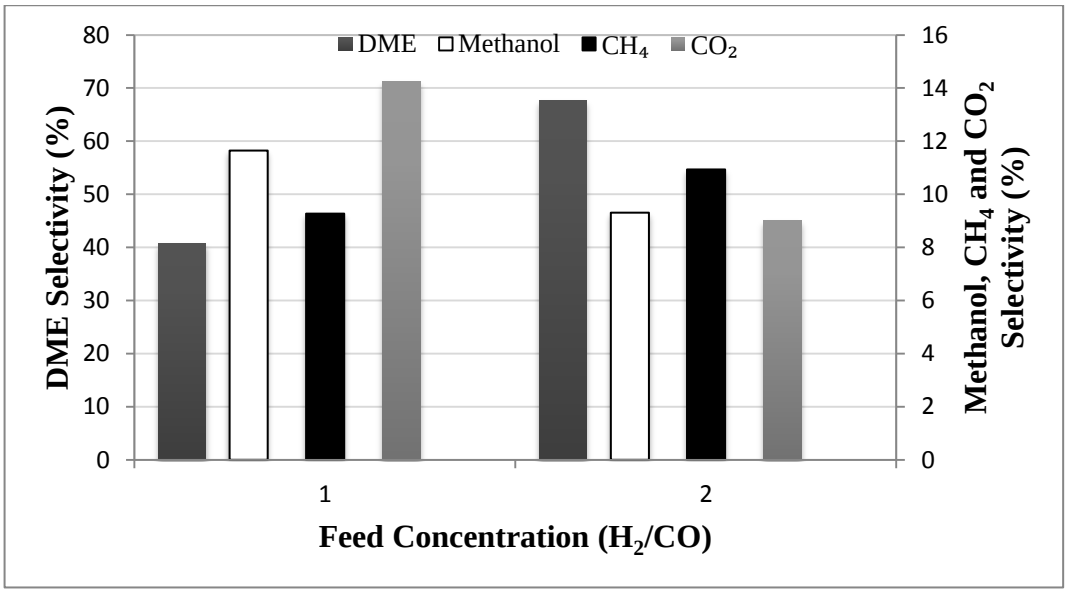

Figure 4.16. Effect of H_2/CO ratio of DME, methanol, CH_4 and CO_2selectivities for HiFUEL R120-10% CeO_2/δ-Al_2O_3(300 ^oC, 34 bar).

Table 4.19. Selectivity of main products with HiFUEL R120-10% CeO_2/δ-Al_2O_3 at different inlet H_2/CO ratios (300 ^oC, 34 bar).

Feed Composition (H_2/CO)	DME selectivity (%)	Methanol selectivity (%)	CH_4 selectivity (%)	CO_2 selectivity (%)
1	40.8	11.6	9.3	14.3
2	67.7	9.3	10.9	9.0

Table 4.20. Yield of main products with HiFUEL R120-10% CeO_2/δ-Al_2O_3 at different inlet H_2/CO ratios (300 ^oC, 34 bar).

Feed Composition (H_2/CO)	DME yield (%)	Methanol yield (%)	CH_4 yield (%)	CO_2 yield (%)
1	3.5	2.0	1.6	2.5
2	10.0	2.8	3.1	2.6

Table 4.21. Yield of by-products with HiFUEL R120-10 % CeO_2/δ-Al_2O_3 at different inlet H_2/CO ratios (300 ^oC, 34 bar).

Feed Composition (H_2/CO)	C_2H_4 yield (%)	C_2H_6 yield (%)	C_3H_8 yield (%)	C_4H_{10} yield (%)	C_5H_{12} yield (%)
1	7.3×10^{-2}	6.9×10^{-1}	5.1×10^{-1}	2.3×10^{-1}	1.1×10^{-2}
2	1.0×10^{-2}	8.3×10^{-2}	1.4×10^{-1}	7.3×10^{-2}	1.0×10^{-2}

4.4. Effect of Catalyst Loading

The results presented in Figures 4.17a and 4.17b show that CO conversion decreases progressively with ceria loading at 275 and 300 ^{o}C, respectively. A similar trend is also observed for DME selectivity, which was found to decrease slowly upon increasing ceria loading from 5 to 10%, but then rapidly by further increasing loading to 20% (Figures 4.18a and 4.18b). These findings are in alignment with the negative impact of basicity on DME production and on CO conversion. Decreased DME production slows down the consumption of methanol, which would thermodynamically reduce the driving force for methanol synthesis and hinder conversion of CO. This phenomenon also explains the increase in methanol selectivity with ceria loading at both temperatures. Apart from this scenario, it is reported that CeO_2 provides a favorable reaction pathway to methanol synthesis [68]. It is also found that exothermic pre-hydrogenation of ceria generates Ce^{3+}centers, which accelerates the CO_2 adsorption and favors hydrogenation of CO_2 into methanol ($CO_2 + 3H_2 \leftrightarrow CH_3OH$) [69]. Although it is not as notable as that of methanol, methane selectivity is also found to increase with ceria loading, possibly either due to hydrogenation of some of the CO (i.e. $CO + 3H_2 \leftrightarrow CH_4 + H_2O$) or post dehydration of DME into hydrocarbons, including mostly methane [70].

The effect of ceria loading on water-gas shift, hence on the product distribution can be traced by the formation of CO_2. It is worth noting that the primary source of CO_2 in the reaction network is water-gas shift. The results presented in Figures 4.18a and 4.18b show that ceria loading promotes CO_2 selectivity which are found to be slightly higher at 275 ^{o}C. These outcomes clearly support water-gas shift promotion by ceria, and the elevated selectivity of CO_2 with temperature is a thermodynamic verification of the fact that CO_2 is coming from water-gas shift. The expected contribution of increased extent of water-gas shift would be via the consumption of H_2O, which would thermodynamically promote methanol dehydration and subsequent DME synthesis. However, the outcomes that show a negative correlation between DME selectivity and ceria loading imply that the expected promotion of DME formation via H_2O removal is not significant. For convenience, product selectivity and CO conversion for all of the catalyst types and for each operating temperature are presented in Figure 4.19.

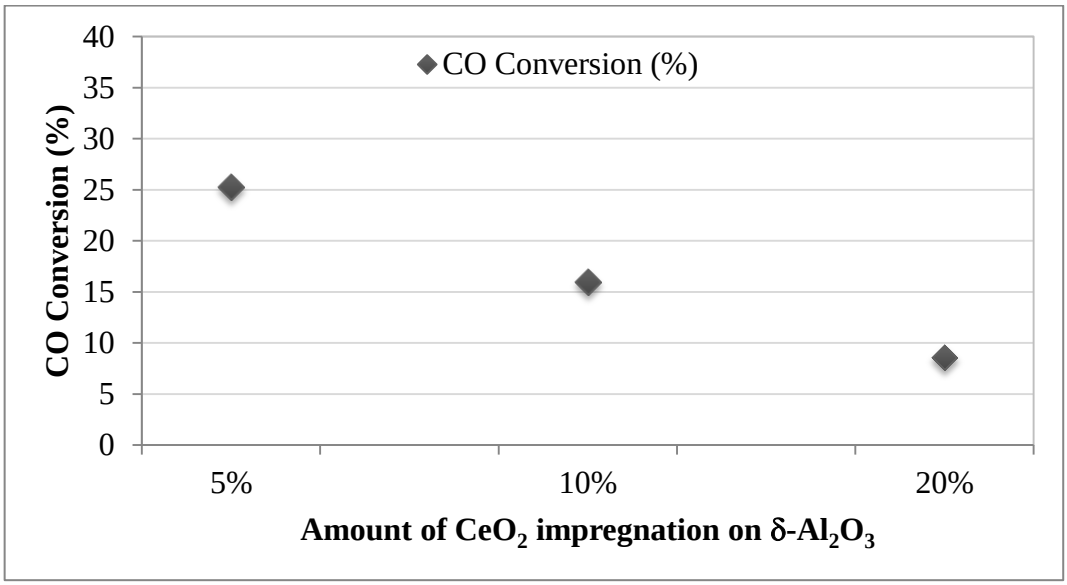

(a)

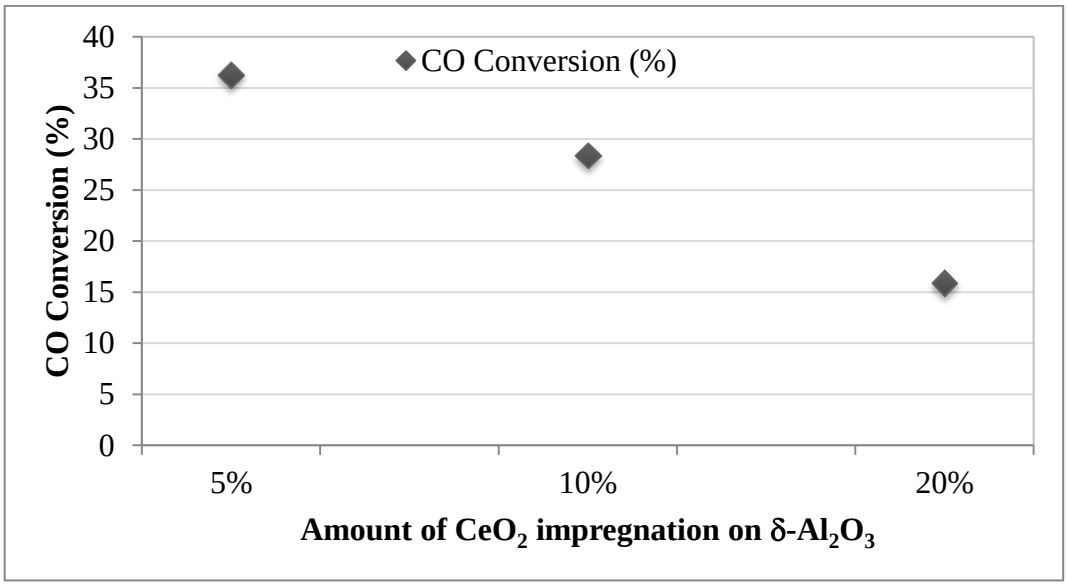

(b)

Figure 4.17. Comparison of catalytic activity of HiFUEL R120-5% CeO_2/δ-Al_2O_3, HiFUEL R120-10% CeO_2/δ-Al_2O_3 and HiFUEL R120-20% CeO_2/δ-Al_2O_3 at (a) 275 ^oC and (b) 300 ^oC ($CO/H_2/N_2$ =32/64/4, 34 bar).

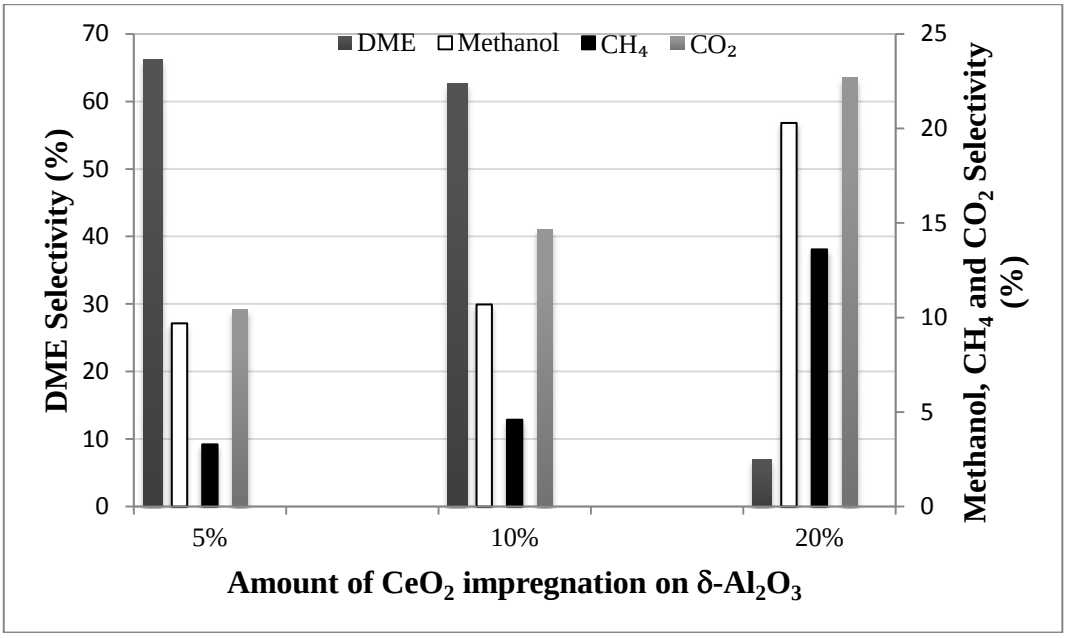

(a)

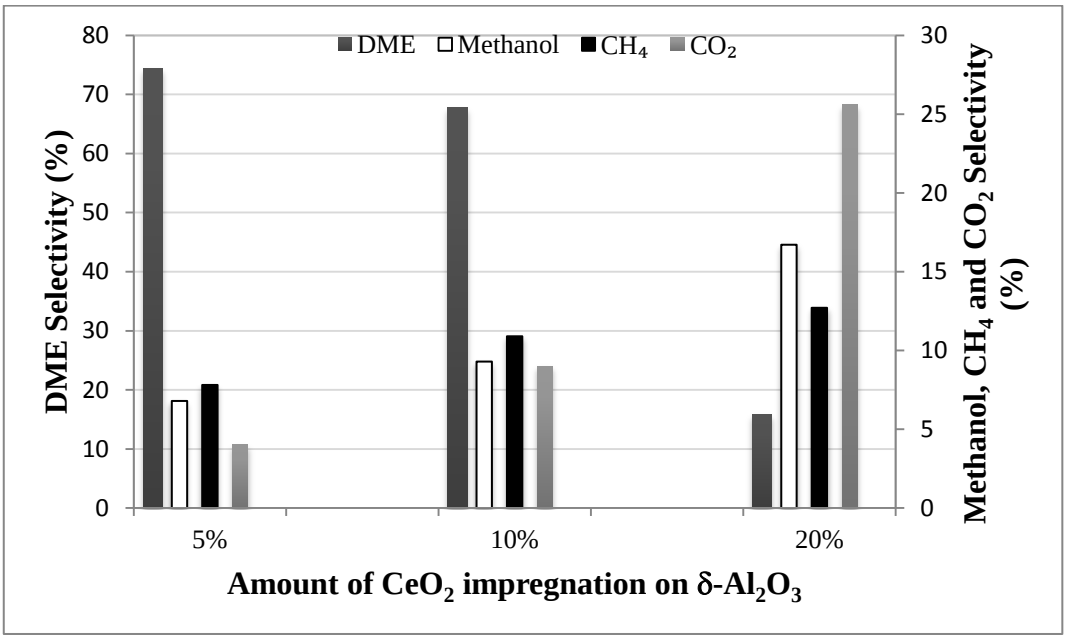

(b)

Figure 4.18. Comparison of DME, methanol, CH_4 and CO_2 selectivity of HiFUEL R120-5% CeO_2/δ-Al_2O_3, HiFUEL R120-10% CeO_2/δ-Al_2O_3 and HiFUEL R120-20% CeO_2/δ-Al_2O_3 at (a) 275 ^oC and (b) 300 ^oC ($CO/H_2/N_2$ =32/64/4, 34 bar).

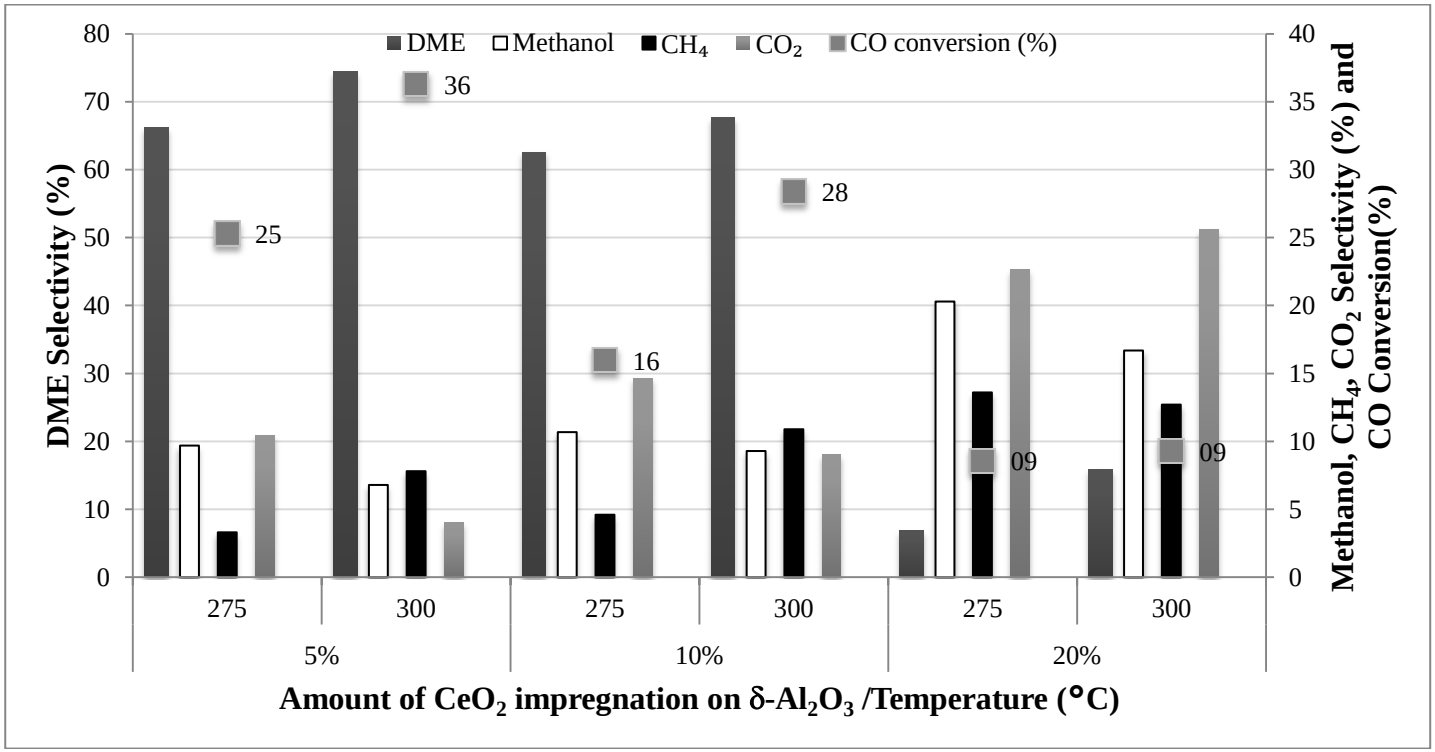

Figure 4.19. Comparison of DME, methanol, CH_4 and CO_2 selectivity, and CO Conversion of HiFUEL R120-5% CeO_2/δ-Al_2O_3, HiFUEL R120-10% CeO_2/δ-Al_2O_3 and HiFUEL R120-20% CeO_2/δ-Al_2O_3 at 275 ^oC and 300 ^oC ($CO/H_2/N_2$ =32/64/4, 34 bar).

5. CONCLUSION

5.1. Conclusions

In this study, the bi-functional DME synthesis catalyst system consisting of the commercial methanol synthesis catalyst HiFUEL-R120 and the methanol dehydration catalyst $CeO_2/\delta\text{-}Al_2O_3$ was examined for direct syngas-to-DME conversion. Three $CeO_2/\delta\text{-}Al_2O_3$ catalysts with various CeO_2 loadings were prepared by the incipient-to-wetness impregnation method. Dual catalyst bed configurations were created in the fixed bed micro-reactor by the sequential loading of methanol synthesis and methanol dehydration catalysts according to the direction of feed flow.

The experimental part of this work consists of a parametric study of DME synthesis from CO hydrogenation as a function of time, temperature, pressure, feed composition and effect of CeO_2 loading on $\delta\text{-}Al_2O_3$. Reaction temperatures of 250, 275 and 300^oC and total pressures of 25 and 34 bar were tested along with CeO_2 loadings of 5%, 10% and 20% CeO_2 on $\delta\text{-}Al_2O_3$ for methanol dehydration. The 5% and 10% $CeO_2/\delta\text{-}Al_2O_3$catalysts were tested in the dual-bed reactor at reaction temperatures of 250, 275 and 300 ^oC at a constant total pressure of 34 bar and H_2/CO molar ratio of 2 in the feed. These catalysts were also examined by varying the pressure at 25 and 34 bar using H_2/CO molar feed ratios of both 1 and 2. Furthermore, 5%, 10% and 20% $CeO_2/\delta\text{-}Al_2O_3$catalysts were compared to observe the effect of CeO_2 loading at reaction temperatures of 275 and 300 ^oC at a constant pressure of 34 bar and a H_2/CO molar ratio of 2. The major outcomes of this study can be summarized as follows:

- Increasing the reaction temperature leads to a gradual increase in CO conversion in dual beds with the 5% or 10% $CeO_2/\delta\text{-}Al_2O_3$catalystas the methanol dehydration component; therefore, optimum temperature is selected as 300 ^oC. However, when 20% $CeO_2/\delta\text{-}Al_2O_3$is used, temperature increase does not affect CO conversion to any extent, which is presumably caused by catalyst deactivation by metal sintering.

- Increasing the reaction pressure also leads to enhanced catalytic activity over 5% and 10% $CeO_2/\delta\text{-}Al_2O_3$, and highest DME selectivity achieved at 34 bar and 300 ^oC with a H_2/CO ratio of 2 are 74.4% and 67.7%, respectively.

- Effect of H_2/CO molar ratio is found to be an effective parameter in DME synthesis where H_2-rich reaction mixtures promote CO conversion and hence increase DME selectivity. Optimum H_2/CO molar ratio in the feed is 2.

- Catalytic activity in terms of CO conversion and DME selectivity both increase as the amount of CeO_2 loading on $\delta\text{-}Al_2O_3$ decreases. The most likely reason is the increase in the acidic sites desirable for methanol dehydration as CeO_2 is known to increase surface basicity.

- Yields of the methanol intermediate, CO_2, CH_4 and other byproduct alkanes reported in each experiment indicate that they affect DME selectivity levels to some extent.

- Among all catalyst systems tested in this study, the Cu-Zn based commercial methanol synthesis catalyst HiFUEL R120 coupled with 5% $CeO_2/\delta\text{-}Al_2O_3$as the methanol dehydration catalyst delivers the highest levels of CO conversion (36%) and DME selectivity (74.4%) at 34 bar, 300 ^oC with a H_2/CO molar feed ratio of 2.

5.2. Recommendations

By taking the results obtained from this parametric study into account, the following recommendations can be valuable for future studies on direct DME synthesis from syngas:

- In order to eliminate possible errors resulting from the assumptions made in estimation and analysis of product distributions, calibrations for all components of the product mixture are highly desirable.

- Catalyst characterization by SEM and EDX can be made to discover the surface morphology of the catalysts for better evaluation of the results obtained.

- Methanol dehydration catalysts may be modified to achieve higher surface acidity.

- CO/CO_2 feed composition may be studied by adding CO_2 in order to observe the effect of CO_2 on product distributions.

- In situ H_2O removal by adsorption can be carried out for eliminating the possible negative effect of excess water in the medium.

- A wider range of operating pressures can be used to observe possible thermodynamic limitations for enhanced CO conversion.

- The optimum ratio of the amount of methanol synthesis and methanol dehydration catalysts in the dual bed configuration can be investigated

REFERENCES

1. Ogawa, T., N. Inoue, T. Shikada and Y. Ohno, "Direct Dimethyl Ether Synthesis", *Journal of Natural Gas Chemistry*, Vol. 12, No. 4, pp. 219–227, 2003.

2. Khandan, N., M. Kazemeini, and M. Aghaziarati, "Direct production of dimethyl ether from synthesis gas utilizing bifunctional catalysts", *Applied Petrochemical Research*, Vol. 1, No. 1–4, pp. 21–27, 2012.

3. Arcoumanis, C., C. Bae, R. Crookes, and E. Kinoshita, "The potential of di-methyl ether (DME) as an alternative fuel for compression-ignition engines: A review", *Fuel*, Vol. 87, No. 7, pp. 1014–1030, 2008.

4. Ju, F., H. Chen, X. Ding, H. Yang, X. Wang, S. Zhang, and Z. Dai, "Process simulation of single-step dimethyl ether production via biomass gasification", *Biotechnology Advances*, Vol. 27, No. 5, pp. 599–605, 2009.

5. Brown, D. M., B. L. Bhatt, T. H. Hsiung, J. J. Lewnard, and F. J. Waller, "Novel technology for the synthesis of dimethyl ether from syngas", *Catalysis Today*, Vol. 8, No. 3, pp. 279–304, 1991.

6. Sofianos, A. C. and M. S. Scurrell, "Conversion of synthesis gas to dimethyl ether over bifunctional catalytic systems", *Industrial and Enginnering Chemistry Research*, Vol. 30, No. 11, pp. 2372–2378, 1991.

7. Azizi, Z., M. Rezaeimanesh, T. Tohidian, and M. R. Rahimpour, "Dimethyl ether: A review of technologies and production challenges", *Chemical Engineering and Process: Process Intensification*, Vol. 82, pp. 150–172, 2014.

8. Ge, X., S. Hu, and Q. Sun, "Surface Acidity/Basicity and Catalytic Reactivity of CeO_2/-Al_2O_3 Catalysts for the Oxidative Dehydrogenation of Ethane with Carbon Dioxide to Ethylene", *Journal of Natural Gas Chemistry*, Vol. 12, No. 3, pp. 119–122, 2003.

9. Doğu, T. and D. Varişli, "Alcohols as alternatives to petroleum for environmentally clean fuels and petrochemicals", *Turkish Journal of Chemistry*, Vol. 31, No. 5, pp. 551–567, 2007.

10. Erdener, H., A. Arinan, and S. Orman, "Future fossil fuel alternative; di-methyl ether (DME) a review", *International Journal of Renewable Energy Resources*, Vol. 1, No. 4, pp. 252–258, 2011.

11. Semelsberger, T. A., R. L. Borup, and H. L. Greene, "Dimethyl ether (DME) as an alternative fuel", *Journal of Power Sources*, Vol. 156, No. 2, pp. 497–511, 2006.

12. Asthana, S., C. Samanta, A. Bhaumik, and B. Banerjee, "Direct synthesis of dimethyl ether from syngas over Cu-based catalysts : Enhanced selectivity in the presence of MgO", *Journal of Catalysis*, Vol. 334, pp. 89–101, 2016.

13. Shikada, T., Y. Ohno, T. Ogawa, M. Ono, M. Mizuguchi, K. Tomura, and K. Fujimoto, "Direct synthesis of dimethyl ether form synthesis gas", *Journal of Natural Gas Chemistry*, Vol. 119, pp. 219–227, 2003.

14. Shukla, M. K., T. Bhaskar, A. K. Jain, S. K. Singal, and M. O. Garg, "Bio-Ethers as Transportation Fuel: A Review", *Indian Institute of Petroleum Dehradun*, pp. 1–40.

15. Wang, M. Q. and H. S. Huang, "A Full Fuel-Cycle Analysis of Energy and Emissions Impacts of Transportation Fuels Produced from Natural Gas", *U.S. Department of Energy*, No. 40, p. 88, 1999.

16. Jun, K.-W., W.-J. Shen, and K.-W. Lee, "Concurrent Production of Methanol and Dimethyl Ether from Carbon Dioxide Hydrogenation : Investigation of Reaction

Conditions", *Bulletin of the Korean Chemical Society*, Vol. 20, No. 9, pp. 993–998, 1999.

17. Sun, J., G. Yang, Y. Yoneyama, and N. Tsubaki, "Catalysis chemistry of dimethyl ether synthesis", *ACS Catalysis*, Vol. 4, No. 10, pp. 3346–3356, 2014.

18. Lee, S., W. Cho, and E. Yoon, "Simulation of fixed bed reactor for dimethyl ether synthesis", *Korean Journal of Chemical Engineering*, Vol. 23, No.4, pp. 522–530, 2006.

19. Lu, W.-Z., L.-H. Teng, and W.-D. Xiao, "Theoretical Analysis of Fluidized-Bed Reactor for Dimethyl Ether Synthesis from Syngas", *International Journal of Chemical Reaction Engineering*, Vol. 1, 2003.

20. Takeguchi, T., K. Yanagisawa, T. Inui, and M. Inoue, "Effect of the property of solid acid upon syngas-to-dimethyl ether conversion on the hybrid catalysts composed of Cu–Zn–Ga and solid acids", *Applied Catalysis A: General*, Vol. 192, No. 2, pp. 201–209, 2000.

21. Lima, S. H., A. M. S. Forrester, L. Amparo Palacio, and A. C. Faro, "Niobia-alumina as methanol dehydration component in mixed catalyst systems for dimethyl ether production from syngas", *Applied Catalysis A: General*, Vol. 488, pp. 19–27, 2014.

22. Jin, D., B. Zhu, Z. Hou, J. Fei, H. Lou, and X. Zheng, "Dimethyl ether synthesis via methanol and syngas over rare earth metals modified zeolite Y and dual Cu-Mn-Zn catalysts", *Fuel*, Vol. 86, No. 17–18, pp. 2707–2713, 2007.

23. Mao, D., W. Yang, J. Xia, B. Zhang, and G. Lu, "The direct synthesis of dimethyl ether from syngas over hybrid catalysts with sulfate-modified γ-alumina as methanol dehydration components", *Journal of Molecular Catalysis A: Chemical*, Vol. 250, No. 1–2, pp. 138–144, 2006.

24. Bozga, G., I. T. Apan, and R. E. Bozga, "Dimethyl Ether Synthesis Catalysts, Processes and Reactors", *Recent Patents Catalysis*, Vol. 2, No. 1, pp. 68–81, 2013.

25. Joo, O. S., K. D. Jung, and S. H. Han, "Modification of H-ZSM-5 and γ-alumina with formaldehyde and its application to the synthesis of dimethyl ether from syn-gas", *Bulletin of the Korean Chemical Society*, Vol. 23, No. 8, pp. 1103–1105, 2002.

26. Kang, S. H., J. W. Bae, H. S. Kim, G. M. Dhar, and K. W. Jun, "Enhanced catalytic performance for dimethyl ether synthesis from syngas with the addition of Zr or Ga on a Cu-ZnO-Al_2O_3/γ- Al_2O_3 bi-functional catalyst", *Energy and Fuels*, Vol. 24, No. 2, pp. 804–810, 2010.

27. Zno, C., O. Al, T. Aguayo, J. Eren, D. Mier, M. Arandes, M. Olazar, and J. Bilbao, "Kinetic Modeling of Dimethyl Ether Synthesis in a Single Step on a CuO-ZnO-Al_2O_3/γ-Al_2O_3 catalyst", *Industrial & Engineering Chemistry Research*, Vol. 46, No. 17, pp. 5522–5530, 2007.

28. Sierra, I., M. Olazar, and A. G. Gayubo, "Deactivation of a CuO-ZnO-Al_2O_3 / γ - Al_2O_3 Catalyst in the Synthesis of Dimethyl Ether", *Industrial & Engineering Chemistry Research*, Vol. 47. No. 7, pp. 2238–2247, 2008.

29. Xu, M., J. H. Lunsford, D. W. Goodman, and A. Bhattacharyya, "Synthesis of dimethyl ether (DME) from methanol over solid-acid catalysts", *Applied Catalysis A General*, Vol. 149, No. 2, pp. 289–301, 1997.

30. Stiefel, M., R. Ahmad, U. Arnold, and M. Döring, "Direct synthesis of dimethyl ether from carbon-monoxide-rich synthesis gas: Influence of dehydration catalysts and operating conditions", *Fuel Processing Technology*, Vol. 92, No. 8, pp. 1466–1474, 2011.

31. Ramos, F. S., A. M. D. D. Farias, L. E. P. Borges, J. L. Monteiro, M. A. Fraga, E. F. Sousa-Aguiar and L. G. Appel, "Role of dehydration catalyst acid properties on one-

step DME synthesis over physical mixtures", *Catalysis Today*, Vol. 101, No. 1, pp. 39–44, 2005.

32. Kang, S. H., J. W. Bae, K. W. Jun and H. S. Potdar, "Dimethyl ether synthesis from syngas over the composite catalysts of Cu-ZnO-Al_2O_3/Zr-modified zeolites", *Catalysis Communications*, Vol. 9, No. 10, pp. 2035–2039, 2008.

33. Xu, Q., T. Li and Y. Yan, "Effects of CaO-modified zeolite on one-step synthesis of dimethyl ether", *Journal of Fuel Chemistry and Technology*, Vol. 36, No. 2, pp. 176–180, Dec. 2008.

34. Cai, M., V. Subramanian, V. V. Sushkevich, V. V. Ordomsky, and A. Y. Khodakov, "Effect of Sn additives on the CuZnAl–HZSM-5 hybrid catalysts for the direct DME synthesis from syngas", *Applied Catalysis A : General*, Vol. 502, pp. 370–379, 2015.

35. Lee, Y. J., M. H. Jung, J. B. Lee, K. E. Jeong, H. S. Roh, Y. W. Suh, and J. W. Bae, "Single-step synthesis of dimethyl ether from syngas on Al_2O_3-modified CuO-ZnO-Al_2O_3/ferrierite catalysts: Effects of Al_2O_3 content", *Catalysis Today*, Vol. 228, pp. 175–182, 2014.

36. Song, F., Y. Tan, H. Xie, Q. Zhang, and Y. Han, "Direct synthesis of dimethyl ether from biomass-derived syngas over Cu–ZnO–Al_2O_3–ZrO_2(x)/γ-Al_2O_3 bifunctional catalysts: Effect of Zr-loading", *Fuel Process. Technology*, Vol. 126, pp. 88–94, 2014.

37. Migliori, M., A. Aloise, and G. Giordano, "Methanol to dimethylether on H-MFI catalyst: The influence of the Si/Al ratio on kinetic parameters", *Catalysis Today*, Vol. 227, pp. 138–143, 2014.

38. Jiang, S., J. Hwang, T. Jin, T. Cai, W. Cho, and S. Park, "Dehydration of Methanol to Dimethyl Ether over ZSM-5 Zeolite", *Bulletin of the Korean Chemical Society*, Vol. 25, No. 2, pp. 185–189, 2004.

39. Wang, Y., W. Wang, Y. Chen, J. Ma, and R. Li, "Synthesis of dimethyl ether from syngas over core–shell structure catalyst CuO–ZnO–Al_2O_3@SiO_2–Al_2O_3", *Chemical Engineering Journal*, Vol. 250, pp. 248–256, 2014.

40. Matsumura, Y., W. Shen, Y. Ichihashi, and M. Okumura, "Low-Temperature Methanol Synthesis Catalyzed over Ultrafine Palladium Particles Supported on Cerium Oxide", Vol. 272, pp. 267–272, 2001.

41. Imamura, S., K. Denpo, K. Utani, Y. Matsumura, and H. Kanai, "Synthesis of methanol over Pd promoted by ceria", *Reaction Kinetics and Catalysis Letters*, Vol. 67, No. 1, pp. 163–168, 1999.

42. Xie, Q., P. Chen, P. Peng, S. Liu, P. Peng, B. Zhang, Y. Cheng, Y. Wan, Y. Liu, and R. Ruan, "Single-step synthesis of DME from syngas on CuZnAl–zeolite bifunctional catalysts: the influence of zeolite type", *RSC Advances*, Vol. 5, No. 33, pp. 26301–26307, 2015.

43. Montesano, R., A. Narvaez, and D. Chadwick, "Shape-selectivity effects in syngas-to-dimethyl ether conversion over Cu/ZnO/Al_2O_3 and zeolite mixtures: Carbon deposition and by-product formation", *Applied Catalysis : A General*, Vol. 482, pp. 69–77, 2014.

44. Fei, J., Z. Hou, B. Zhu, H. Lou, and X. Zheng, "Synthesis of dimethyl ether (DME) on modified HY zeolite and modified HY zeolite-supported Cu-Mn-Zn catalysts", *Applied Catalysis : A General*, Vol. 304, No. 1–2, pp. 49–54, 2006.

45. Yoo, K. S., J. H. Kim, M. J. Park, S. J. Kim, O. S. Joo, and K. D. Jung, "Influence of solid acid catalyst on DME production directly from synthesis gas over the admixed catalyst of Cu/ZnO/Al_2O_3 and various SAPO catalysts", *Applied Catalysis : A General*, Vol. 330, No. 1–2, pp. 57–62, 2007.

46. Moradi, G. R., S. Nosrati, and F. Yaripor, "Effect of the hybrid catalysts preparation method upon direct synthesis of dimethyl ether from synthesis gas", *Catalysis Communications*, Vol. 8, No. 3, pp. 598–606, 2007.

47. Ahmad, R., D. Schrempp, S. Behrens, J. Sauer, M. Döring, and U. Arnold, "Zeolite-based bifunctional catalysts for the single step synthesis of dimethyl ether from CO", *Fuel Processing Technology*, Vol. 121, pp. 38–46, 2014.

48. Khoshbin, R. and M. Haghighi, "Direct conversion of syngas to dimethyl ether as a green fuel over ultrasound-assisted synthesized CuO-ZnO-Al_2O_3/HZSM-5 nanocatalyst: effect of active phase ratio on physicochemical and catalytic properties at different process conditions", *Catalysis Science Technology*, Vol. 4, No. 6, pp. 1779–1792, 2014.

49. Phienluphon, R., K. Pinkaew, G. Yang, J. Li, Q. Wei, Y. Yoneyama, T. Vitidsant, and N. Tsubaki, "Designing core (Cu/ZnO/Al_2O_3)–shell (SAPO-11) zeolite capsule catalyst with a facile physical way for dimethyl ether direct synthesis from syngas", *Chemical Engineering Journal*, Vol. 270, pp. 605–611, 2015.

50. Martínez, A., "Study of the interaction between components in hybrid CuZnAl / HZSM-5 catalysts and its impact in the syngas-to-DME reaction", *Catalysis Today*, Vol. 179, No. 1, pp. 43–51, 2012.

51. Khoshbin, R. and M. Haghighi, "Direct syngas to DME as a clean fuel: The beneficial use of ultrasound for the preparation of CuO–ZnO–Al_2O_3/HZSM-5 nanocatalyst", *Chemical Engineering Research and Design*, Vol. 91, No. 6, pp. 1111–1122, 2013.

52. Li, Z., J. Li, M. Dai, Y. Liu, D. Han, and J. Wu, "The effect of preparation method of the Cu–La_2O_3–ZrO_2/γ-Al_2O_3 hybrid catalysts on one-step synthesis of dimethyl ether from syngas", *Fuel*, Vol. 121, pp. 173–177, 2014.

53. Nie, R., H. Lei, S. Pan, L. Wang, J. Fei, and Z. Hou, "Core-shell structured CuO-ZnO@H-ZSM-5 catalysts for CO hydrogenation to dimethyl ether", *Fuel*, Vol. 96, pp. 419–425, 2012.

54. Vishwanathan, V., H.-S. Roh, J.-W. Kim, and K.-W. Jun, "Surface Properties and Catalytic Activity of TiO_2–ZrO_2 Mixed Oxides in Dehydration of Methanol to Dimethyl Ether", *Catalysis Letters*, Vol. 96, No. 1/2, pp. 23–28, 2004.

55. Moradi, G. R., F. Yaripour, and P. Vale-Sheyda, "Catalytic dehydration of methanol to dimethyl ether over mordenite catalysts", *Fuel Processing Technology*, Vol. 91, No. 5, pp. 461–468, May 2010.

56. Cho, W., T. Song, A. Mitsos, J. T. McKinnon, G. H. Ko, J. E. Tolsma, D. Denholm, and T. Park, "Optimal design and operation of a natural gas tri-reforming reactor for DME synthesis", *Catalysis Today*, Vol. 139, No. 4, pp. 261–267, 2009.

57. Huang, M.-H., H.-M. Lee, K.-C. Liang, C.-C. Tzeng, and W.-H. Chen, "An experimental study on single-step dimethyl ether (DME) synthesis from hydrogen and carbon monoxide under various catalysts", *International Journal of Hydrogen Energy*, Vol. 40, No. 39, pp. 13583-13593, 2015.

58. Ereña, J., R. Garoña, J. M. Arandes, A. T. Aguayo, and J. Bilbao, "Effect of operating conditions on the synthesis of dimethyl ether over a CuO-ZnO-Al_2O_3/NaHZSM-5 bifunctional catalyst", *Catalysis Today*, Vol. 107–108, pp. 467–473, 2005.

59. Mao, D., W. Yang, J. Xia, B. Zhang, Q. Song, and Q. Chen, "Highly effective hybrid catalyst for the direct synthesis of dimethyl ether from syngas with magnesium oxide-modified HZSM-5 as a dehydration component", *Journal of Catalysis*, Vol. 230, No. 1, pp. 140–149, 2005.

60. Yoo, K. S., J.-H. Kim, M.-J. Park, S.-J. Kim, O.-S. Joo, and K.-D. Jung, "Influence of solid acid catalyst on DME production directly from synthesis gas over the admixed catalyst of $Cu/ZnO/Al_2O_3$ and various SAPO catalysts", *Applied Catalysis: A General*, Vol. 330, pp. 57–62, 2007.

61. Xu, Q. L., T. C. Li, and Y. J. Yan, "Effects of CaO-modified zeolite on one-step synthesis of dimethyl ether", *Journal of Fuel Chemistry and Technology*, Vol. 36, No. 2, pp. 176–180, 2008.

62. Avci, A. K., "Computational and Experimental Investigation of Catalytic Hydrocarbon Fuel Processing for Autothermal Hydrogen Production," Ph. D. Dissertation, Boğaziçi University, 2003.

63. Yildirim, R., "Pyrolysis and Oxidative Pyrolysis of Chloromethane (natural gas)", Ph. D Thesis, University of California, 1993.

64. Kevan, L. and J. A. Beran, "Molecular Electron Ionization Cross Sections at 70 eV", The Journal of Physical Chemistry, Vol. 73, No. 11, pp. 3866-3876, 1966.

65. Hudson, J. E., M. L. Hamilton, C. Vallance, and P. W. Harland, "Absolute Electron Impact Ionization Cross-sections for the C1 to C4 Alcohols", Physical Chemistry Chemical Phsyics, Vol. 5, No.15, pp. 3162–3168, 2003.

66. Mardanpour, M. M., R. Sadeghi, M. R. Ehsani, and M. Nasr Esfahany, "Enhancement of dimethyl ether production with application of hydrogen-permselective Pd-based membrane in fluidized bed reactor", *Journal of Industrial and Engineering Chemistry*, Vol. 18, No. 3, pp. 1157–1165, 2012.

67. Chen, H. J., C. W. Fan, and C. S. Yu, "Analysis, synthesis, and design of a one-step dimethyl ether production via a thermodynamic approach", *Applied Energy*, Vol. 101, pp. 449–456, 2013.

68. Ereña, J., I. Sierra, M. Olazar, A. G. Gayubo, and A. T. Aguayo, "Deactivation of a CuO-ZnO-Al_2O_3/γ-Al_2O_3 Catalyst in the Synthesis of Dimethyl Ether", *Industrial and Engineering Chemistry Research*, Vol. 47, No. 7, pp. 2238–2247, 2008.

69. Shen, W. J., Y. Ichihashi, and Y. Matsumura, "Methanol Synthesis from Carbon Monoxide and Hydrogen over Ceria-Supported Copper Catalyst Prepared by a Coprecipitation Method", *Catalysis Letters* Vol. 83, No. 1, pp. 33–35, 2002.

70. Graciani, J., K. Mudiyanselage, F. Xu, a. E. Baber, J. Evans, S. D. Senanayake, D. J. Stacchiola, P. Liu, J. Hrbek, J. F. Sanz, and J. a. Rodriguez, "Highly active copper-ceria and copper-ceria-titania catalysts for methanol synthesis from CO_2", *Science*, Vol. 345, No. 6196, pp. 546–550, 2014.

71. Mao, D., W. Yang, J. Xia, B. Zhang, Q. Song, and Q. Chen, "Highly effective hybrid catalyst for the direct synthesis of dimethyl ether from syngas with magnesium oxide-modified HZSM-5 as a dehydration component", *Journal of Catalysis*, Vol. 230, No. 1, pp. 140–149, 2005.

APPENDIX A: SAMPLE CONVERSION, SELECTIVITY AND YIELD CALCULATIONS

In this parametric study the results of the tests are analyzed via an online connection with GC 2014 and GCMS-QP2010. Calibration curves for both analyzing systems are achieved by either online calibration or injection. In this Appendix, sample calculations for CO conversion and selectivity are given in details for the run with HiFUEL R120-5% CeO_2/δ-Al_2O_3 at 300 ^oC, 34 bar and total reactant gas flow rate as 100 ml/min having a feed composition of CO/H_2/N_2 as 32/64/4 with 0.2 g HiFUEL R120 and 0.2 g 5% CeO_2/δ-Al_2O_3.

The CO conversion is calculated according to the Eq 3.1 which is as follows:

$$X_{CO}\ (\%)\ =\ \left[\frac{n_{CO,in}-n_{CO,out}}{n_{CO,in}}\right]\times 100 \tag{3.1}$$

Steady state is achieved around 1 hour after the reaction gasses are fed to the system. Therefore average of the five successive data used in the calculations. Molar flow rate of the CO at the inlet and outlet at one run is calculated from peak areas recorded from GC analyses as 6.5 μmol/min and 3.8 μmol/min for $n_{CO,in}$ and $n_{CO,out}$, respectively. For every run $n_{CO,out}$ hence $X_{CO}(\%)$ is calculated. Average of the conversions is taken as the overall conversion for this experiment. Thus according to Equation 3.1 the CO conversion is found as 36.3%.

$$X_{CO}(\%) = \left[\frac{6.52-3.79}{6.52}\right]\times 100 = 41.87\%$$

Selectivity of the CH_4 and CO_2 is found from Equation 3.2 and Equation 3.3 where the overall selectivity is defined as the ratio of moles of CO converted to a specific component to total moles of CO converted to products.

$$S_{CO_2}(\%) = \left[\frac{n_{CO_2}}{n_{CO,in} - n_{CO,out}}\right] \times 100 \quad (3.2)$$

$$S_{CH_4}(\%) = \left[\frac{n_{CH_4}}{n_{CO,in} - n_{CO,out}}\right] \times 100 \quad (3.3)$$

GC and GC-MS are calibrated for both CH_4 and CO_2 therefore their molar flow rate is calculated from both systems and the results are found to be in consistent. From the GC molar flow rates of n_{CH_4} and n_{CO_2} in the outlet stream is achieved as 0.11 μmol/min and 0.13 μmol/min, respectively. From the GC-MS flow rates of n_{CH_4} and n_{CO_2} in the outlet stream is achieved as 0.10 μmol/min and 0.19 μmol/min, respectively. The selectivity calculations for these products are carried out data taken from the GC-MS since all of the other products can be only detected from GC-MS. Thus selectivity for CH_4 and CO_2 is found as 3.66 and 7.31 μmol/min, respectively.

$$S_{CO_2}(\%) = \left[\frac{0.19}{6.52 - 3.79}\right] \times 100 = 7.31\%$$

$$S_{CH_4}(\%) = \left[\frac{0.10}{6.52 - 3.79}\right] \times 100 = 3.66\%$$

The presence of DME, methanol and other paraffins was detected by GC-MS, but their yield and selectivity calculations necessitate calibrations for individual components. However, GC-MS calibration for these molecules was not so easy since GC-MS detector became saturated during analyzing the high purity substances. Due to the unavailability of standard mixtures that could be used for calibration, molar flow rates methanol and other paraffins of were calculated with following equation [62];

$$n_i = n_{ref} \frac{M_{ref}}{M_i} \frac{A_{ref}}{A_i} \frac{Q_{ref}}{Q_i} \quad (3.4)$$

where subscript “i” and “ref” correspond to the quantified species and reference compound, respectively. N is the number of moles of species, M is molecular weight and A is the area under the peak obtained from GCMS-QP2010. For methanol and other paraffins, methane is taken as reference compound. Q is total ionization cross section. The response factor could be defined as arbitrary peak area per mole of compound. Since the electron impact voltage of GC-MS is 70 eV, experimental values of total ionization cross sections for ethanol and methane corresponding this voltage were found in literature given in Table 3.7 [63,64].

Table 3.7. Total ionization cross section of the some compounds.

Compound	**Q (Total ionization cross section)**
CH_4	4.67
C_2H_4	6.93
C_2H_6	8.51
C_3H_8	10.5
C_4H_{10}	15.3
C_5H_{12}	18.6
CH_3OH	4.44

At first DME molar flow rate was also calculated from Equation 3.4. However since DME was a main product this approach was not found to be appropriate to use the method given in Equation 3.4 was proposed to quantify only small amounts of by-products whose peak areas are comparable with that of the reference component [62]. Therefore DME flow rate was determined from the carbon balance calculation. Using this method is expected to deliver correct outcomes since almost all of the carbon containing products could be analyzed via GC-MS, and no coke formation was observed over the catalyst within the range of experimental conditions studied. Number of moles of paraffins other than CH_4 was calculated by Equation 3.4. Therefore, molar flow rate of

the DME is obtained according to Equation 3.5 and 3.6 where N denotes the number of Carbon in the compound and n as molar flow rate of that compound.

$$\mathrm{N_{DME}n_{DME}} = \left[(\mathrm{N_{CO}n_{CO,in}} - \mathrm{N_{CO}n_{CO,out}}) - (\mathrm{N_{CH_4}n_{CH_4}} + \mathrm{N_{CO_2}n_{CO_2}} + \mathrm{N_{CH_4OH}n_{CH_4OH}} + \sum \mathrm{N_{Paraffins}n_{Paraffins}})\right] \quad (3.5)$$

$$\sum \mathrm{N_{Paraffins}n_{Paraffins}} = \mathrm{N_{C_2H_4}n_{C_2H_4}} + \mathrm{N_{C_2H_6}n_{C_2H_6}} + \mathrm{N_{C_3H_8}n_{C_3H_8}} + \mathrm{N_{C_4H_{10}}n_{C_4H_{10}}} + \mathrm{N_{C_5H_{12}}n_{C_5H_{12}}} \quad (3.6)$$

Therefore according Equation 3.4 $n_{C_2H_4}$ is calculated as follows;

$Q_{CH_4} = 4.67$

$Q_{C_2H_4} = 6.93$

$M_{CH_4} = 16.1\ g/mol$

$M_{C_2H_4} = 28.1\ g/mol$

$A_{CH_4} = 3799711$

$A_{C_2H_4} = 4605618$

n_{CH_4}=0.1 µmol/min

$$n_{C_2H_4} = 0.1 \times \frac{16.1}{28.1} \times \frac{3799711}{4605618} \times \frac{4.67}{6.93} = 3.18 \times 10^{-2}\ \mu\text{mol/min}$$

Molar flow rate of other paraffins are also calculated with the same way according to Equation 3.4.

$$\sum \mathrm{N_{Paraffins}n_{Paraffins}} = 2 \times 3.18 \times 10^{-2} + 2 \times 5.22 \times 10^{-3} + 3 \times 2.03 \times 10^{-2} + 4 \times 3.61 \times 10^{-3} + 5 \times 3.99 \times 10^{-3} = 0.64$$

$$n_{DME} = \frac{[(1 \times 6.52 - 1 \times 3.79) - (1 \times 0.10 + 1 \times 0.19 + 1 \times 0.17 + 0.64)]}{2}$$

$$= 0.94\ \mu mol/min$$

Selectivity of DME is calculated as given in the Equation 3.7.

$$S_{DME}\,(\%) = \left[\frac{2 \times n_{DME}}{n_{CO,in} - n_{CO,out}}\right] \times 100 \tag{3.7}$$

$$S_{DME}\,(\%) = \left[\frac{2 \times 0.94}{6.52 - 3.79}\right] \times 100 = 68.7\%$$

Yield of the products are also calculated from the Equation 3.8 as follows:

$$Y_i = \frac{n_i}{n_{CO,in}} \times 100 \tag{3.8}$$

$$Y_{DME} = \frac{0.94}{6.52} \times 100 = 14.4\%$$